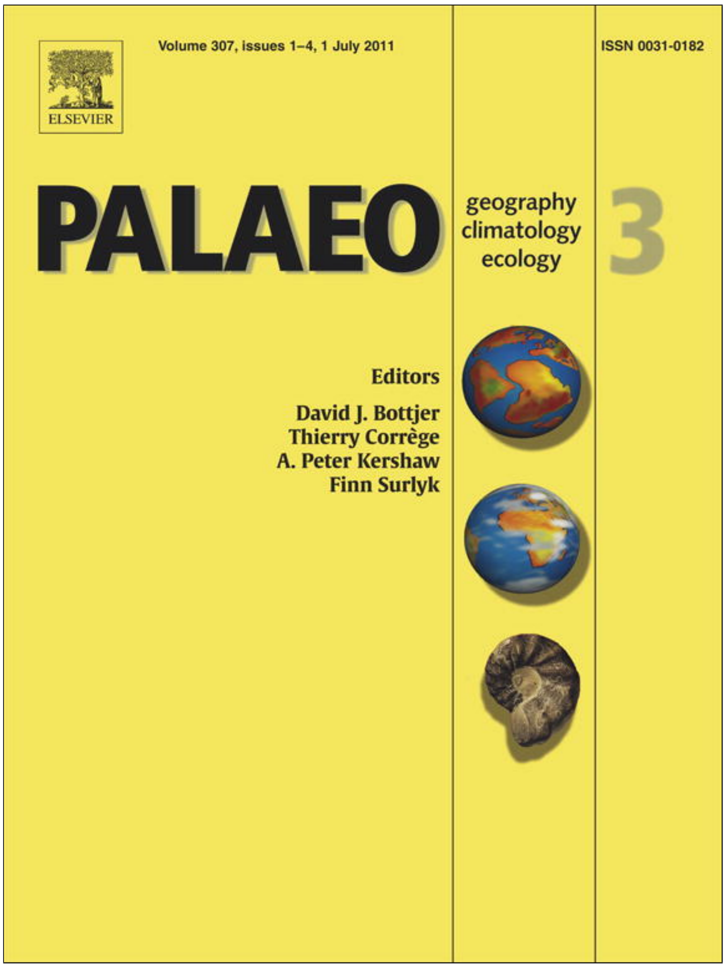
ELSEVIER
Volume 307, issues 1–4, 1 July 2011
ISSN 0031-0182
PALAEO
geography
climatology
ecology
3
Editors
David J. Bottjer
Thierry Corrège
A. Peter Kershaw
Finn Surlyk

Palaeogeography, Palaeoclimatology, Palaeoecology 307 (2011) 1–16

Contents lists available at ScienceDirect

Palaeogeography, Palaeoclimatology, Palaeoecology

journal homepage: www.elsevier.com/locate/palaeo

Stratigraphic evidence for the Hirnantian (latest Ordovician) glaciation in the Zagros Mountains, Iran

Mohammad Ghavidel-syooki [a], J. Javier Álvaro [b,*], Leonid Popov [c], Mansoureh Ghobadi Pour [d], Mohammad H. Ehsani [a], Anna Suyarkova [e]

[a] Institute of Petroleum Engineering, Technical Faculty of Tehran University, P.O. Box 11365-4563, Tehran, Iran
[b] Centre of Astrobiology (CSIC/INTA), Ctra. de Torrejón a Ajalvir km 4, 28850 Torrejón de Ardoz, Spain
[c] Department of Geology, Natural Museum of Wales, Cardiff, Cathays Park, Cardiff CF10 3NP, Wales, UK
[d] Department of Geology, Faculty of Sciences, Golestan University, Gorgan 49138-15739, Iran
[e] Department of Stratigraphy and Palaeontology, Russian Geological Research Institute (VSEGEI), 74 Sredniy prospect, 199106 St. Petersburg, Russia

ARTICLE INFO

Article history:
Received 11 November 2010
Received in revised form 28 March 2011
Accepted 13 April 2011
Available online 20 April 2011

Keywords:
Diamictite
Black shale
Unconformity
Arabian Plate
Gondwana

ABSTRACT

High-latitude Hirnantian diamictites (Dargaz Formation) and lower-Silurian kerogenous black shales (Sarchahan Formation) are locally exposed in the Zagros Mountains. The glaciogenic Dargaz deposits consist of three progradational/retrogradational cycles, each potentially controlled by the regional advance and retreat of the Hirnantian ice sheet. Glacial incisions of sandstone packages change laterally from simple planar to high-relief (<40 m deep) scalloped truncating surfaces that join laterally forming complex polyphase unconformities that scour into the underlying Seyahou Formation. The glaciated source area was to the present-day west, in the region of the Arabian Shield, where numerous tunnel valleys have been reported. Based on a study of palynomorphs and graptolites, the glaciomarine Dargaz diamictites are dated as Hirnantian, whereas the youngest Sarchahan black shales are diachronous throughout the Zagros, ranging from the Hirnantian *persculptus* to the earliest Aeronian (Llandovery) *triangulatus* zones. The diachronism is related to onlapping geometries capping an inherited glaciogenic palaeorelief that preserved different depth incisions and source areas. Our data suggest the presence of Hirnantian satellite ice caps adjacent the Zagros margin of Arabia and allow us to fill a gap in the present knowledge of the peripheral extension of the Late Ordovician ice sheet.

1. Introduction

Although Upper Ordovician, ice-proximal strata have been reported from Saudi Arabia (McClure, 1978,1988; Vaslet, 1989,1990; McGillivray and Husseini, 1992; Senalp and Al-Laboun, 2000; Senalp et al., 2002; Melvin et al., 2003,2004; Clark-Lowes, 2005; Moscariello et al., 2008) and neighbouring regions, such as Oman (Hughes-Clark, 1988), Jordan (Armstrong et al., 2005; Turner et al., 2005; Armstrong et al., 2009), and Turkey (Monod et al., 2003; Ghienne et al., 2010), the peripheral extension of the Hirnantian ice sheet in the Arabian margin of Gondwana is still controversial. The onset of Hirnantian tunnel valley networks allows a differentiation between the 'areas closest to the ice centre' (Algeria, Arabia, Jordan, Libya, and Mauritania; Ghienne, 2003; Le Heron et al., 2004; Ghienne et al., 2007; Armstrong et al., 2009) and 'ice-marginal areas' (e.g., Morocco and Turkey; Monod et al., 2003; Le Heron et al., 2007). Le Heron and Dowdeswell's (2009) argued that several separate ice sheets developed throughout North Gondwana, and not that a continuous ice sheet straddled North Africa-Arabia, South Africa, and South America. The existence of some satellite ice caps, sited on upland areas during the Hirnantian, has been recognised in platforms fringing North Gondwana (e.g., Le Heron et al., 2007; Álvaro and Van Vliet-Lanoë, 2009; Gutiérrez-Marco et al., 2010), but no data were yet available from the Zagros fold-thrust belt fringing the Arabian Plate.

Lower Silurian shales across North Africa, the Arabian Peninsula, and the Persian Gulf include organically enriched intervals that have been argued to be the source of 90% of the regions' early Palaeozoic oil (Lüning et al., 2000,2005; Le Heron et al., 2009). Two intervals, Rhudanian and Telychian–Wenlockian in age, are commonly referred to 'hot shales' and are characterised by elevated TOC values and a pronounced 'kick' on gamma ray logging tools (Lüning et al., 2005). Hirnantian tunnel valleys in Arabia, up to 400 m deep and 80 km wide, also represent an important reservoir target in the subsurface, potentially sealed by the rich petroleum source rocks of the Silurian graptolitic shales (Melvin et al., 2003).

The aim of this paper is threefold: (i) to analyse, based on outcrop data, the available Hirnantian profiles in the Zagros Mountains and to provide their basic sequence framework for the Ordovician–Silurian

* Corresponding author.
E-mail addresses: m_ghavidelsyooki@yahoo.com (M. Ghavidel-syooki), jjalvaro@unizar.es (J.J. Álvaro), Leonid.Popov@museumwales.ac.uk (L. Popov), m.ghobadipour@gu.ac.ir (M.G. Pour), mh_ehsani@hotmail.com (M.H. Ehsani), Anna_Suyarkova@vsegei.ru (A. Suyarkova).

0031-0182/$ – see front matter © 2011 Elsevier B.V. All rights reserved.
doi:10.1016/j.palaeo.2011.04.011

transition; (ii) to correlate them with the well-known succession in Saudi Arabia and Jordan; and (iii) to discuss the ice sheet distribution in the Arabian margin of Gondwana.

2. Geological setting and lithostratigraphy

The Zagros Mountains are a fold-thrust belt located in the northeastern margin of the Arabian Plate. The latter is bounded to the northeast by the Zagros Main Thrust Fault (ZMTF in Fig. 1A), to the northwest by the Dead Sea Fault Zone (DSFZ), to the southwest by the Red Sea rift margin (RSRM), and to the southeast by the Indian Ocean passive margin (IOPM) (Alavi, 2004; Sepehr and Cosgrove, 2004; Sherkati et al., 2006). In the Zagros Mountains, Ordovician–Silurian rocks crop out only in two massifs, north of Bandar Abbas (Fig. 1B), named Kuh-e Faraghan and Kuh-e Gahkum (Wolfart, 1981; Davoudzadeh et al., 1986; Mobasheri, 2005). They represent the stratotypes of the Seyahou, Dargaz, and Sarchahan formations (Fig. 2).

2.1. Seyahou Formation

This unit, introduced by Ghavidel-syooki and Khosravi (1995) and ca. 870 m thick in the Kuh-e Faraghan stratotype, consists of greenish and black shales with intercalations of thin sandstone, conglomerate, and carbonate siltstone (Fig. 2). Its lower contact is faulted and its top is marked by an erosive unconformity. Three members can be distinguished: (i) a lower conglomeratic unit, 20 m thick, composed of polymictic conglomerate beds alternating with thin shale intervals; (ii) a middle heterolithic member, 460 m thick, composed of shale/sandstone alternations bearing interbedded phosphatic and bioclastic carbonate siltstone, which have yielded a rich and diversified shelly fauna, composed of trilobites, bryozoans, calcitic and linguliformean brachiopods, molluscs, and conodonts; and (iii) an upper member, 390 m thick, recognisable by thin-bedded, rhythmic claystone/sandstone couplets extremely rich in ichnofossils. The entire formation has been assigned to the middle Floian–Katian based on the occurrence of the conodont *Baltoniodus triangularis* (Lindström) in the lowermost part of the formation, the trilobites *Neseuretinus turcicus* Dean and *Dalmanitina* cf. *acuta* Hammann and the brachiopod *Svobodaina havliceki* Villas, in the middle part of the formation (this study). In addition to the shelly fauna, the Seyahou shale interbeds have yielded well-preserved acritarchs and chitinozoans, which allow identification of a biostratigraphical succession ranging from the latest Floian *Euconochitina brevis* Zone to the latest Katian *Ancyrochitina merga* Zone (Ghavidel-syooki, 2000; and this work).

2.2. Dargaz Formation

The formation, here erected and 10–70 m thick in the Kuh-e Faraghan stratotype, consists of whitish sandstones and structureless to diffusely laminated diamictites, which form two diamictite/sandstone couplets (Fig. 2; see formal definition in Appendix A). Both the lower and upper contacts are erosive unconformities. The formation is poorly exposed but easily distinguishable and mappable at the southeast corner of the Kuh-e Faraghan massif. The Hirnantian age of the formation will be discussed in Section 3.

2.3. Sarchahan Formation

The formation, introduced by Ghavidel-syooki (1995), ranges from 56 to 90 m in Kuh-e Faraghan to 170 m in the Kuh-e Gahkum stratotype. It consists of a monotonous, black to greyish shale succession with interbedded thin-bedded conglomerates, sandstones and dolostones, and embedded centimetre- to metre-thick carbonate concretions (Fig. 2). Its erosive top is marked by the occurrence of the channelled conglomerates of the Devonian Zakeen Formation. The Silurian age of

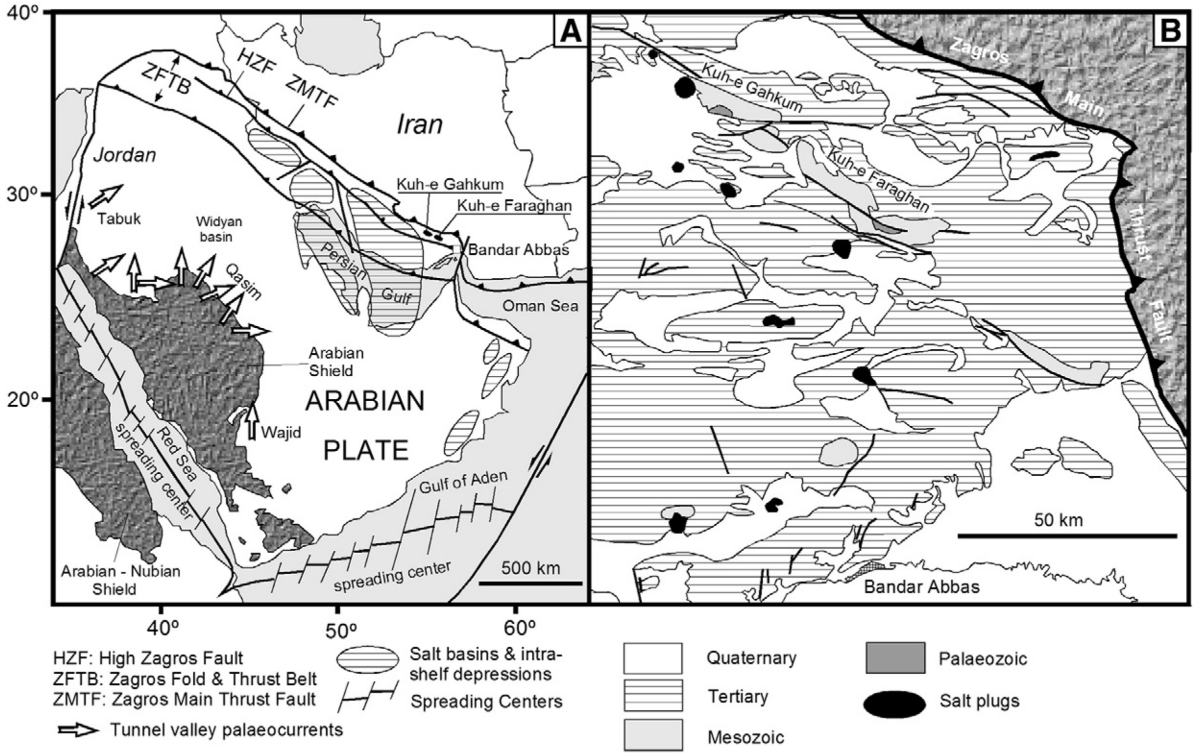

Fig. 1. A. Major tectonic features of the Arabian Plate, the Zagros Mountains, and adjacent areas; modified from Heydari (2008); tunnel-valley palaeocurrents from Vaslet (1989, 1990), Clark-Lowes (2005), Melvin et al. (2003), and Moscariello et al. (2008). B. Geological map of the study areas in the southeastern Zagros Fold and Thrust Belt, North of Bandar Abbas; modified from Afaghi and Salek (1977).

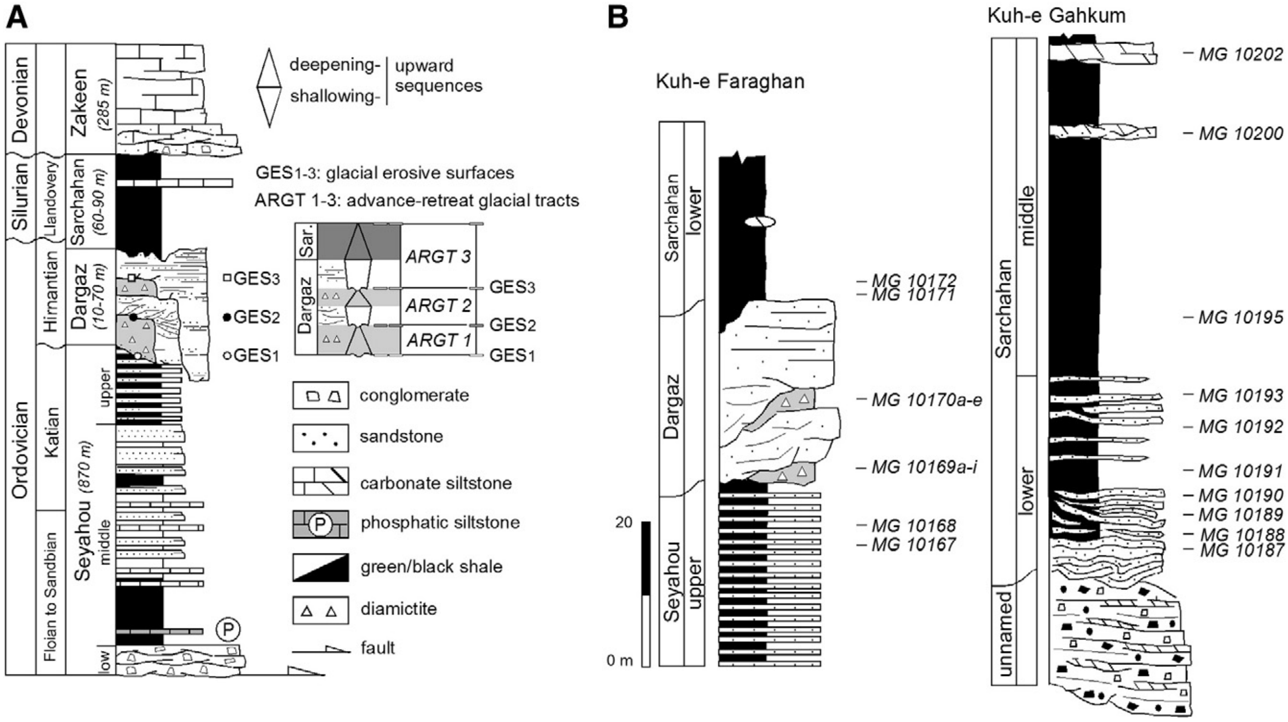

Fig. 2. A. Lower Palaeozoic stratigraphic units of Kuh-e Faraghan and sequence framework of the Hirnantian Dargaz Formation, Zagros Mountains; GES sensu Le Heron et al. (2010). B. Stratigraphic logs of the Hirnantian–Llandovery transition at Kuh-e Faraghan and Kuh-e Gakhum with location of the sampled fossiliferous horizons reported in the text.

the Sarchahan Formation has been documented by the presence of graptolites (Berry and Boucot, 1972; Wolfart, 1981; Alsharhan and Nairn, 1997; Rickards et al., 2000), acritarchs and chitinozoans (Ghavidel-syooki and Khosravi, 1995; Ghavidel-syooki, 2000; Ghavidel-syooki and Winchester-Seeto, 2004). At Kuh-e Gahkum, more than 100 m of Silurian black shales have residual TOC values ranging between 1.0% and 4.3%, this being high for an overmature source rock that has reached the graphite stage. Their δ^{13}C values (ca. −30.8‰) are comparable to those of other Silurian shales from Oman and Saudi Arabia. Palinspastic reconstructions indicate that the Silurian shales at Kuh-e Gahkum have been buried to at least 6 km during the Pliocene, preceding the main phase of the Zagros Orogeny (Bordenave and Burwood, 1990; Jones and Stump, 1999).

It is assumed that the Sarchahan Formation participated in the genesis of the huge gas accumulations found in the Permo-Triassic Dalan and Kangan formations (former Khuff Formation) and underlying strata, in Iran, Qatar, and Abu Dhabi (Bordenave and Burwood, 1990; Mahmoud et al., 1992; Bordenave, 2008). It is speculated that the Suru (a few kilometres west of Bandar Abbas) and Salakh (Qeshm Island) gas accumulations were probably sourced from these lower Silurian shales (Ala et al., 1980).

3. Biostratigraphic control

Both the Dargaz diamictites and the basal Sarchahan black shales have been palaeontologically sampled in order to check a possible diachronism in their lithostratigraphic contacts. Their palynomorphs (mainly chitinozoans and acritarchs) and graptolites were determined. The latter are housed in the F.N. Chernyshev Central Scientific-Research Geological Exploration Museum, St. Petersburg, Russia (acronym: CNIGR).

3.1. Chitinozoans

The chitinozoan-based biostratigraphy of the Ordovician–Silurian boundary interval in the Zagros Mountains was first outlined by Ghavidel-syooki (2000) and Ghavidel-syooki and Winchester-Seeto (2004). These studies revealed the presence of chitinozoans characteristic of: (i) the Katian *Armoricochitina nigerica* and *Ancyrochitina merga* zones in the upper part of the Seyahou Formation; and (ii) the late Hirnantian to early Rhudddanian *Spinachitina fragilis* Zone in the lower part of the Sarchahan Formation at Kuh-e Faraghan. The chitinozoan assemblages also support a broad 'North' Gondwanan biogeographic affinity, in particular by comparison with those of Maghreb (North Africa) and the Arabian Plate (for details, see Paris, 1990; Paris et al., 2000a, 2000b; Webby et al., 2004).

A new sampling has revealed that, despite the common record of erosive unconformities, a complete succession of Late Ordovician chitinozoan zones is preserved at Kuh-e Faraghan. The preservation of chitinozoans in that stratigraphic interval is usually fairly poor and they comprise a relatively minor component in relation to other palynomorphs. Nevertheless, some distinctive taxa of the high-latitude peri-Gondwanan Hirnantian chitinozoan assemblage zones are present, including *Armoricochitina nigerica* (Bouché), *Spinachitina oulebsiri* Paris, Bourahrouh and Le Hérissé, *Belonechitina pseudarabiensis* Butcher, *Calpichitina lenticularis* Bouché, *Desmochitina minor* Eisenack, Bourahrouh and Le Hérissé, and *Tanuchitina* cf. *elongata* Bouché (Fig. 3; Table 1).

The *Tanuchitina elongata* Zone is defined by the occurrence of the eponymous (and index) species, which appears in the horizon MG10169c, about 3 m above the base of the lower Dargaz diamictite (Fig. 2). The associated assemblage includes *Armoricochitina nigerica*, *Calpichitina lenticularis*, *Euconochitina* sp., and *Lagenochitina baltica* Eisenack. The stratigraphic ranges of all these taxa cross the Seyahou/Dargaz contact. *Desmochitina minor* occurs in a single sample (horizon MG10169c) in the middle part of the lower Dargaz diamictite. The upper Dargaz diamictite (horizons MG10170a, MG10170c) contains an oligotaxic association that includes *Tanuchitina* cf. *elongata*, *A. nigerica*, *Belonechitina pseudarabiensis*, and *C. lenticularis*.

The *Spinachitina oulebsiri* Zone is defined in the section by the first appearance (FAD) of the index species in the upper part of the upper Dargaz diamictite (horizon MG10170d) in association with

Belonechitina pseudarabiensis Butcher and *Cyathochitina caputoi* Da Costa (Fig. 3). *B. pseudarabiensis* was described originally from the Silurian Mudawwara Formation of Jordan, where it is confined to the *ascensus–acuminatus* graptolite zones (Butcher, 2009). Data from Kuh-e Faraghan suggest that this species has a wider range and is transitional from the Hirnantian to the Rhuddanian. *C. caputoi* is represented by specimens with a typical short and thick carina (for further discussion, see Grahn, 2006; Butcher, 2009).

Butcher (2009) suggested that *Spinachitina oulebsiri* represents a junior synonym of *Spinachitina fragilis* (Nestor, 1980). Alternatively, Vandenbroucke et al. (2009) suggested that the Ordovician–Silurian boundary interval may contain several morphologically similar *Spinachitina* species and suggested that *S. fragilis* should be restricted to the Rhuddanian. There is little doubt that the taxonomy of the *Spinachitina* species, which occur across the Ordovician–Silurian transition, requires substantial revision (Vandenbroucke et al., 2009; Delabroye and Vecoli, 2010). The revision of *S. fragilis* by Butcher (2009: text-Fig. 5) based on topotype material from North Estonia, can be considered as an important step in that direction. Until the taxonomy of *Spinachitina fragilis* and related species is resolved, we consider herein *S. oulebsiri* as a separate taxon.

Spinachitina fragilis occurs from the base of the Sarchahan Formation and overlaps, in the lower part of its range, with the uppermost *Normalograptus persculptus* Zone (this was documented in Ghavidel-syooki and Winchester-Seeto, 2004, and has been reconfirmed again across the Ordovician–Silurian boundary interval in Kuh-e Faraghan). Thus data from the Kuh-e Faraghan section may suggest that the FAD of *S. fragilis* takes place in upper Hirnantian strata.

3.2. Acritarchs

All samples from the Dargaz Formation contain abundant and well-preserved acritarchs varying from yellow to orange in colour. There are also a few recycled acritarch taxa including *Coryphidium* sp., *Aureotesta* sp., *Pirea* sp., and *Striatotheca* sp., which occur in the lower Dargaz diamictite (Fig. 4; Table 1). These recycled taxa derived

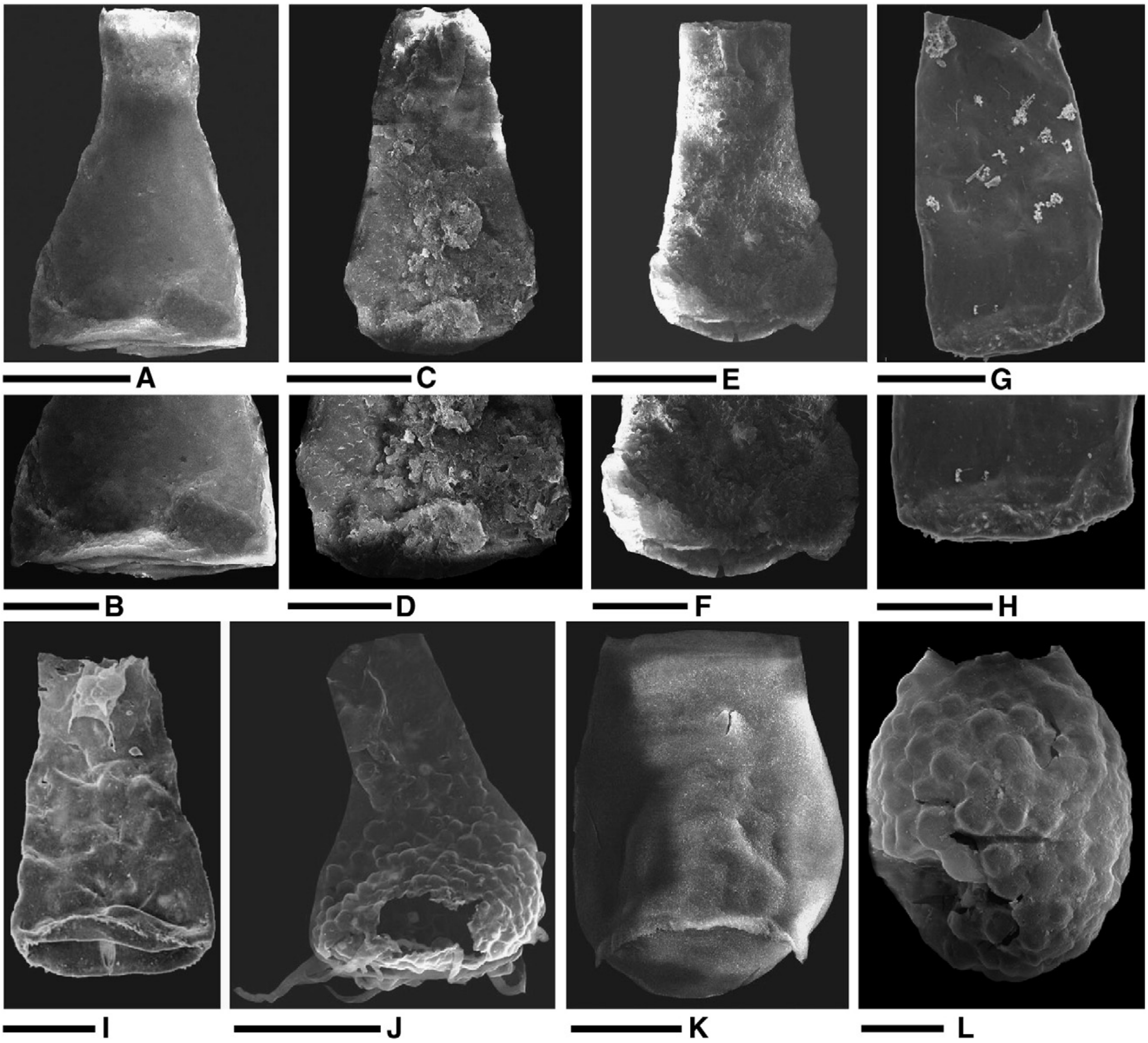

Fig. 3. Representative chitinozoans of the upper part of the Seyahou Formation and the Dargaz diamictites. A–B. *Cyathochitina caputoi*Da Costa, 1971 (latest Hirnantian) from the upper Dargaz diamictite. C–F. *Belonechitina pseudarabiensis*Butcher, 2009 (latest Hirnantian) from the upper Dargaz diamictite. G–I. *Spinochitina oulebsiri* Paris, Bourohrouh and Le Hérissé, 2000 (latest Hirnantian) from the upper Dargaz diamictite. J. *Ancyrochitina merga*Jenkins, 1970 (late Katian) from the upper member of the Seyahou Formation. K. *Armoricochitina nigerica*Bouché, 1965 (Sandbian–early Katian) from Seyahou strata underlying the *merga* zone. L. *Desmochitina minor*Eisenack, 1931(Floian–Hirnantian) from the lower Dargaz diamictite.

Table 1
List of acritarchs (1577 determined specimens, 84.3% in abundance), chitinozoans (167, 8.9%), cryptospores (121, 6.5%), and scolecodonts (6, 0.3%) found in the lower and upper Dargaz diamictites, representative of the Hirnantian *Tanuchitina elongata* and *Spinachitina oulebsiri* zones; grey shades represent the species that exclusively occur in the upper Dargaz diamictite.

Dargaz diamictites	**Lower** (levels 10169)									**Upper** (levels 10170)					total
	a	b	c	d	e	f	g	h	i	a	b	c	d	e	
Acritarchs															
Actinotodissus crassus	2	0	0	2	10	3	5	5	5	15	10	2	0	14	73
Aureotesta sp.	1	0	2	1	0	0	1	1	1	0	1	1	0	0	19
Coryphidium sp. (reworked)	1	0	0	0	0	0	0	0	0	0	0	0	0	0	1
Crassiangulina tessellita	0	0	0	0	3	0	2	0	3	0	0	0	0	0	8
Dactylofusa spinata	2	2	0	2	10	0	3	0	4	10	0	0	0	3	36
Dactylofusa striata	3	5	2	2	3	0	3	0	0	0	0	0	0	5	23
Diexallophasis denticulata	5	2	3	2	15	12	12	7	12	16	12	15	5	16	134
Dorsennidium hamii	0	0	0	0	0	0	5	0	2	10	5	7	0	4	33
Gorgonisphaeridium antiquum	0	0	3	2	8	0	0	0	0	0	0	0	0	0	13
Leiosphaeridia sp.	6	3	9	3	12	0	10	10	10	30	20	15	0	4	132
Multiplicisphaeridium bifurcatum	0	0	0	0	5	2	0	5	3	10	5	2	0	5	37
Neoveryhachium carminae	0	0	0	0	5	0	0	0	0	0	0	0	0	0	5
Othosphaeridium rectangulare	0	0	0	0	0	3	4	0	0	0	0	0	0	2	9
Orthosphaeridium insculptum	0	2	0	0	0	2	3	0	0	4	0	5	0	5	21
Petaloferidium stigii	1	0	0	3	0	0	0	0	0	0	0	0	0	0	4
Polygonium gracile	2	0	0	0	3	1	2	0	1	0	2	0	1	2	14
Striatotheca sp.	2	1	3	2	1	1	2	1	1	2	1	2	0	0	19
Sylvanidium paucibrachium	14	5	6	3	0	0	0	0	0	12	10	10	0	10	70
Tapetisphaerites sp.	0	0	0	0	10	3	10	10	0	10	0	0	0	1	44
Tylotopalla sp.	0	1	1	0	3	0	0	?	2	4	0	2	0	?	13
Veryhachium oklahomense	4	2	3	0	30	3	4	5	6	35	12	11	0	29	144
Veryhachium reductum	0	0	0	0	10	0	7	0	0	0	0	0	0	0	17
Veryhachium subglobosum	12	6	14	2	25	5	5	6	15	55	55	62	0	44	306
Veryhachium triangulatum	2	5	4	5	12	4	7	8	3	30	10	10	0	4	104
Villosacapsula irrorata	3	6	17	3	5	2	4	0	0	15	10	7	0	5	77
Villosacapsula setosapellicula	0	5	12	3	1	6	10	10	8	25	20	14	0	20	134
Dactylofusa ctenista	0	0	?	0	0	0	0	0	0	25	10	12	0	21	68
Dorsennidium undosum	0	0	0	0	0	0	0	0	0	0	0	5	0	0	5
Lophosphaeridium sylvanium	0	0	0	0	0	0	0	0	0	0	5	11	0	0	16
Multiplicisphaeridium irregulare	0	0	0	0	0	0	0	0	0	0	0	3	0	0	3
Pirea sp. (reworked)	0	0	0	0	0	0	0	0	0	0	?	5	0	0	5
Chitinozoans															
Armoricochitina nigerica	0	0	5	4	2	2	4	2	2	3	0	0	0	?	24
Calpichitina lenticularis	0	0	2	0	0	0	2	0	0	0	0	5	0	0	9
Desmochitina minor	0	0	0	0	0	0	1	0	0	0	0	0	0	?	1
Euconochitina sp.	0	0	1	0	0	0	0	0	0	0	0	0	0	0	1
Lagenochitina baltica	0	0	2	0	0	0	4	0	0	0	0	0	0	0	6
Rhabdochitina usitata	0	1	0	0	0	0	0	0	0	0	0	0	0	0	1
Tanuchitina elongata	0	0	4	2	2	0	5	0	3	2	?	5	0	2	25
Belonechitina pseudarabiensis	0	0	0	0	0	0	0	0	0	5	10	20	25	0	60
Cyathochitina caputoi	0	0	0	0	0	0	0	0	0	0	0	0	5	5	10
Spinachitina oulebsiri	0	0	0	0	0	0	0	0	0	0	0	0	30	0	30
Cryptospores	0	12	14	0	7	4	5	?	12	21	25	0	0	21	121
Scolecodonts	0	1	0	0	0	0	5	0	0	0	0	0	0	0	6

most probably from the underlying Seyahou strata and are grey to brown in colour. There is not yet a well established approach to the acritarch biostratigraphy of the Upper Ordovician. As it was mentioned by Vecoli (2008) and Delabroye and Vecoli (2010), in the present state of knowledge, a detailed comparison and correlation of Hirnantian acritarch assemblages from different regions cannot be made unless they are fully illustrated. Most of the acritarch taxa identified from the Dargaz Formation are transitional from the Katian to the Hirnantian and only *Veryhachium triangulatum* Konzalova-Mazancova, *Dactylofusa ctenista* (Loeblich and Tappan), and *Petaloferidium stigii* Jacobson were confined to the Hirnantian in the Upper Ordovician sequence of 'North' Gondwana (Vecoli and Le Hérissé, 2004: Fig. 4). In addition, *Crassiangulina tessellita*Jardiné et al., 1972, previously considered as a Silurian–Late Devonian taxon, has been recorded for the first time in the Hirnantian. *Neoveryhachium carminae* (Cramer) Cramer, 1971, originally a Middle Silurian taxon (although some representatives of the genus occur in the Late Ordovician of North Africa; Molyneux, 1988; Vecoli, 1999), is also recorded for the first time in Hirnantian strata.

The phytoplankton recovered from the Dargaz diamictites contains some common taxa (e.g., *Villosacapsula irrorata* (Loebich and Tappan), *Dactylofusa spinata* (Staplin, Jansonious and Pocock), *Dorsennidium hamii* (Wright and Meyers), *Multiplicisphaeridium* spp., and *Villosacapsula setosapellicula* (Loeblich and Tappan) (Jacobson and Achab, 1985)). This assemblage also occurs in the Late Ordovician 'Assemblage TAS3' of Paris et al. (2007) from the Turkish Taurids, although both diversity and dominant taxa are different. A similar acritarch assemblage was recently documented from the Hirnantian (*Tanuchitina elongata* Zone) upper part of the 'Gorgan Schists' in the Radkan area, south of Kordkuy city, in the north-eastern Alborz Mountains, Iran (Ghavidel-syooki, 2008).

3.3. Graptolites

3.3.1. Kuh-e Faraghan

The occurrence of Hirnantian graptolites in the Sarchahan Formation of Kuh-e Faraghan was first reported by Rickards et al. (2000); however, details of their stratigraphic position were not given. Two horizons (MG10171and MG10172) sampled on the western side of the Tang-e-Pashagh rivulet from the lower 0.4 m of the Sarchahan Formation (intervals 0–0.2 m and 0.2–0.4 m from the base of the formation, respectively; Fig. 2) have yielded a moderately diverse graptolite assemblage, including *Normalograptus ajjeri* (Legrand), *N. parvulus* (Lapworth), *N. medius* (Tornqist), *N. persculptus* (Elles and Wood), *Glyptograptus*? *laciniosus* (Churkin and Carter), *G.*? *lungmaensis* (Sun), *Glyptograptus lanpherei* (Churkin and Carter), *N. wangjiawanensis* (Mu and Lin), *N. rhizinus* (Li and Yang), *N.* ex gr. *normalis* (Lapworth), and *Neodiplograptus* cf. *shanchongensis* (Li) (Fig. 5). This association shows close taxonomic similarities to the graptolite association reported by Xu et al. (2005) from the middle and upper parts of the Hirnantian *Normalograptus persculptus* Zone in the Upper Yangtze Region, South China. It differs, however, in the high abundance of *N. ajjeri* and the rare presence of *N. persculptus*, which is typical of graptolite associations from North African (Legrand, 2001) and Arabian (Loydell, 2007) sectors of Gondwana.

3.3.2. Kuh-e Gahkum

The current knowledge of Silurian graptolites at Kuh-e Gahkum is mainly based on data published by Rickards et al. (2000), who reported the occurrence of a moderately diverse assemblage characteristic of the late Aeronian *Stimulograptus sedgwickii* and *Lituigraptus convolutus* zones. Our study reveals that the lowermost part of the Sarchahan Formation exposed in the area (horizons MG10187a and 10188a) contains graptolites diagnostic of the earliest Aeronian *Demirastrites triangulatus* Zone, previously unreported in the area. This suggests that the age of the base of the Sarchahan Formation at Kuh-e Gahkum is considerably younger than at Kuh-e Faraghan, where it is dated as late Hirnantian. The lowermost horizon MG10187a contains three taxa: *Demirastrites* ex gr. *triangulatus* (Harkness), *Glyptograptus* ex gr. *tamariscus* (Nicholson), and *Pribylograptus*? sp. (Fig. 6C–D, K). The second graptolite-bearing horizon (MG10188a) contains *Demirastrites triangulatus triangulatus* (Harkness), *Demirastrites* cf. *praedecipiens* (Sudburi), *Glyptograptus* ex gr. *tamariscus* (Nicholson), *Neodiplograptus* cf. *sinuatus* (Nicholson), and *Neolagarograptus* sp. (Fig. 6A, B, E–I, L–M, O).

Graptolites of the late Aeronian *Lituigraptus convolutus* Zone have been recovered from a single horizon (MG10192). In addition to the index species of the biozone, the assemblage includes *Rastrites phleoides* Tornquist, *Pristiograptus regularis* (Tornquist), *Petalolithus praecursor* Boucek and Přibyl, *Normalograptus* sp., *Pribylograptus* ex gr. *argutus* (Lapworth), and *Pseudoretiolites* cf. *perlatus* (Nicholson) (Fig. 6J, N, T–U, X–Z).

The graptolite association characteristic of the overlying *Stimulograptus sedgwickii* Zone has been recovered from two horizons (MG10193 and MG10195). The lowermost horizon (MG10193) contains an almost monospecific assemblage dominated by *Neolagarograptus tenuis* (Portlock), in association with subsidiary *Pristiograptus* cf. *variabilis* (Perner) (Fig. 6P–S, V). The graptolite assemblage from horizon MG10195 is also of low diversity, and has yielded abundant *Stimulograptus sedgwickii* (Portlock) and a few specimens of *Pristiograptus* sp. (broad form), *Metaclimacograptus* sp., and "*Monograptus*" cf. *gemmatus* (Barrande) (Fig. 6W, AA–BB).

The Aeronian graptolite fauna recovered from Kuh-e Gahkum is characterised by remarkably low-diversity patterns, in comparison to contemporary faunas from low latitudes (e.g., North America, Baltoscandia, and South China). It shows distinct similarities to the Aeronian graptolite faunas from southwest Libya described by Štorch and Massa (2003, 2006). The most similar is the graptolite association of the *Stimulograptus sedgwickii* Zone, which is characterised by the abundance of the index species; other components of the assemblage (e.g., metaclimacograptids and pristiograptids) are extremely rare. The lower part of the zone displays a characteristic horizon with an oligotaxic association dominated by *Neolagarograptus tenuis*. Elsewhere, the low-diversity graptolite assemblages are typical of Aeronian sections of the North African and Arabian sectors of Gondwana (Štorch and Massa, 2006, pp 90–91).

4. Facies associations and erosive unconformities

The Dargaz Formation is divisible into two diamictite/sandstone couplets, up to 40 m thick. The base of the formation (GES1 in Fig. 2) and the lower contact of both sandstone bodies (GES2–3) represent distinct erosive discontinuities. In the south-eastern corner of the Kuh-e Faraghan massif, and along 2 km, the three GES (glacial erosive surfaces sensu Le Heron et al., 2010) are recognisable (Fig. 7A–C). To the southwest, it is difficult to trace these key surfaces along strike due to thickness variations and apparent truncation against crosscutting overlying units. This is due to the erosive character of the sandstone packages, which can even scour into the underlying Seyahou Formation. These erosive surfaces change laterally from simple planar to high-relief scalloped truncating surfaces to complex polyphase surfaces. As a result, the lower couplet is absent in the south-western corner of the Kuh-e Faraghan massif, where the Dargaz Formation is exclusively represented by the uppermost sandstone bed.

4.1. The Dargaz diamictites

The lower and upper diamictites of the Dargaz Formation form massive to crudely stratified, tabular beds, up to 6 m thick. Scattered granule to pebble-sized, outsized clasts (mainly quartzite lonestones) are either isolated or chaotically clustered and embedded in a greenish, clayey siltstone matrix (Fig. 7D–E). The upper Dargaz diamictite is relatively homogeneous in lithology, whereas the thicker, lower Dargaz diamictite is commonly cut by metre-thick, broadly scoured, sandstone bodies with pervasive low-angle and trough cross-lamination (Fig. 7F), and load and flute casts, which indicate a range of north to northeast-directed palaeocurrents. In thin-section, these consist of a mixture of unsorted, fine- to medium-grained sandstone with relatively high mud content and occasional preservation of granule-sized quartz and quartzite granules 'floating' within a fine-grained matrix (Fig. 8A).

Outsized clasts embedded in massive diamictites represent rain-out processes formed by the settling of suspended fine material and release of coarser dropstones from icebergs in the vicinity of a calving front. Weakly developed lamination may record episodic current activity that resulted from storm, turbidity or wave-influenced processes. Crosscutting channels from the lower Dargaz diamictite represent high-energy episodes, most probably related to ice-proximal outwash deposits, in the form of glaciofluvial or glaciomarine bars.

Fig. 4. Representative acritarchs of the Dargaz diamictites; see Table 1 for stratigraphic setting. A. *Villosacapsula setosapellicula* Loeblich and Tappan, 1976 (Sanbian–Hirnantian). B. *Tylotopalla* sp. (although this genus is abundant in the Silurian, its Hirnantian record was previously reported by Vecoli and Le Hérissé, 2004). C. *Veryhachium subglobosum* Jardiné et al., 1974 (Katian). D. *Sylvanidium paucibrachium* Loeblich, 1970 (late Katian–Hirnantian). E. *Dorsenidium hamii* (Loeblich, 1970) and Stancliffe, 1994 (Sandbian–Hirnantian). F. *Polygonium gracile* Vavdrová, 1966 emend. Sarjeant and Stancliffe, 1994 (Furongian–Devonian). G. *Orthosphaeridium insculptum* Loeblich, 1970 (Sandbian–Hirnantian). H. *Villosacapsula irrorata* (Loeblich and Tappan, 1978) Fensome et al., 1990 (Katian–Hirnantian). I. *Tetrahedraletes* sp. (cryptospore). J. *Veryhachium triangulatum* Konzalova-Mazankova, 1969 (Katian). K. *Villosacapsula setosapellicula* Loeblich and Tappan, 1976. L. *Orthosphaeridium rectangulare* (Eisenack, 1963) Eisenack, 1968 (Darriwillian–Katian). M. *Orthosphaeridium insculptum* Loeblich, 1970 (Sandbian–Hirnantian). N–O. *Crassiangulina tessellita* Jardiné et al., 1972. P. *Diexallophasis denticulata* (Stockmans and Willière, 1962) Loeblich, 1970 (Sandbian–Devonian). Q. *Multiplicisphaeridium bifurcatum* Staplin et al., 1965 (late Sandbian–late Hirnantian). R. *Neoveryhachium carminae* (Cramer) Cramer, 1971 (Katian–middle Wenlockian). S. *Multiplicisphaeridium irregulare* Staplin et al., 1965 (late Sandbian–late Hirnantian). T. *Actinotodissus crassus* Loeblich and Tappan, 1978 (Sandbian–Katian).

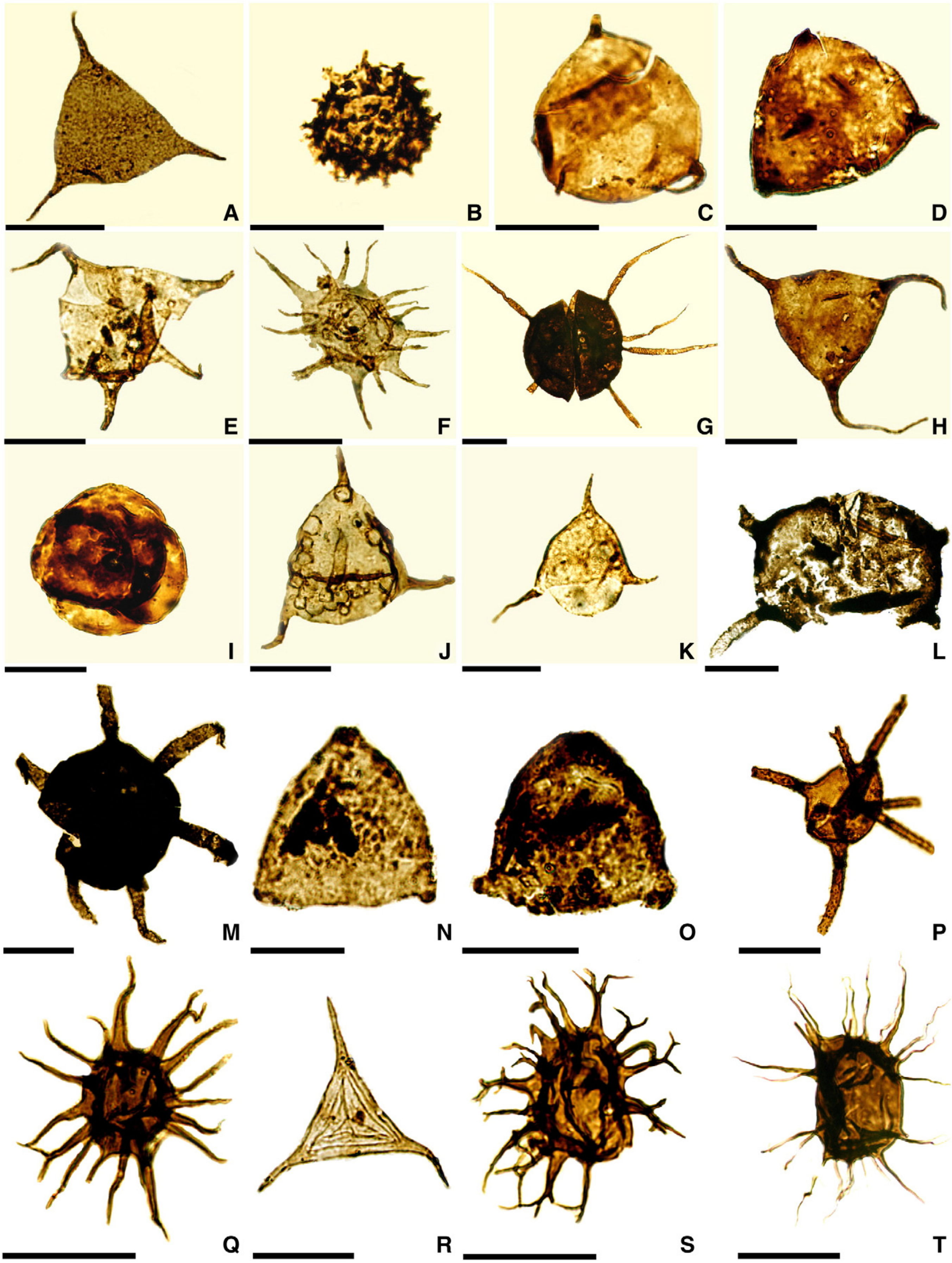
A
B
C
D
E
F
G
H
I
J
K
L
M
N
O
P
Q
R
S
T

4.2. The Dargaz sandstones

Two packages of moderately sorted, fine- to coarse-grained sandstones are recognised in the Dargaz Formation. The lower Dargaz sandstone, up to 15 m thick, consists of 30–80 cm thick, lenticular cross-stratified bedsets with poorly organised palaeocurrent trends. Its base is scoured and locally formed by amalgamation of the sandstone channels described within the lower diamictite. The entire sandstone unit exhibits a coarsening- and thickening-upward trend. By contrast, the upper Dargaz sandstone, up to 30 m thick, consists of scouring and lenticular sandstones passing upward into thin, tabular-bedded, parallel to low-angle laminae. Petrographically, the Dargaz

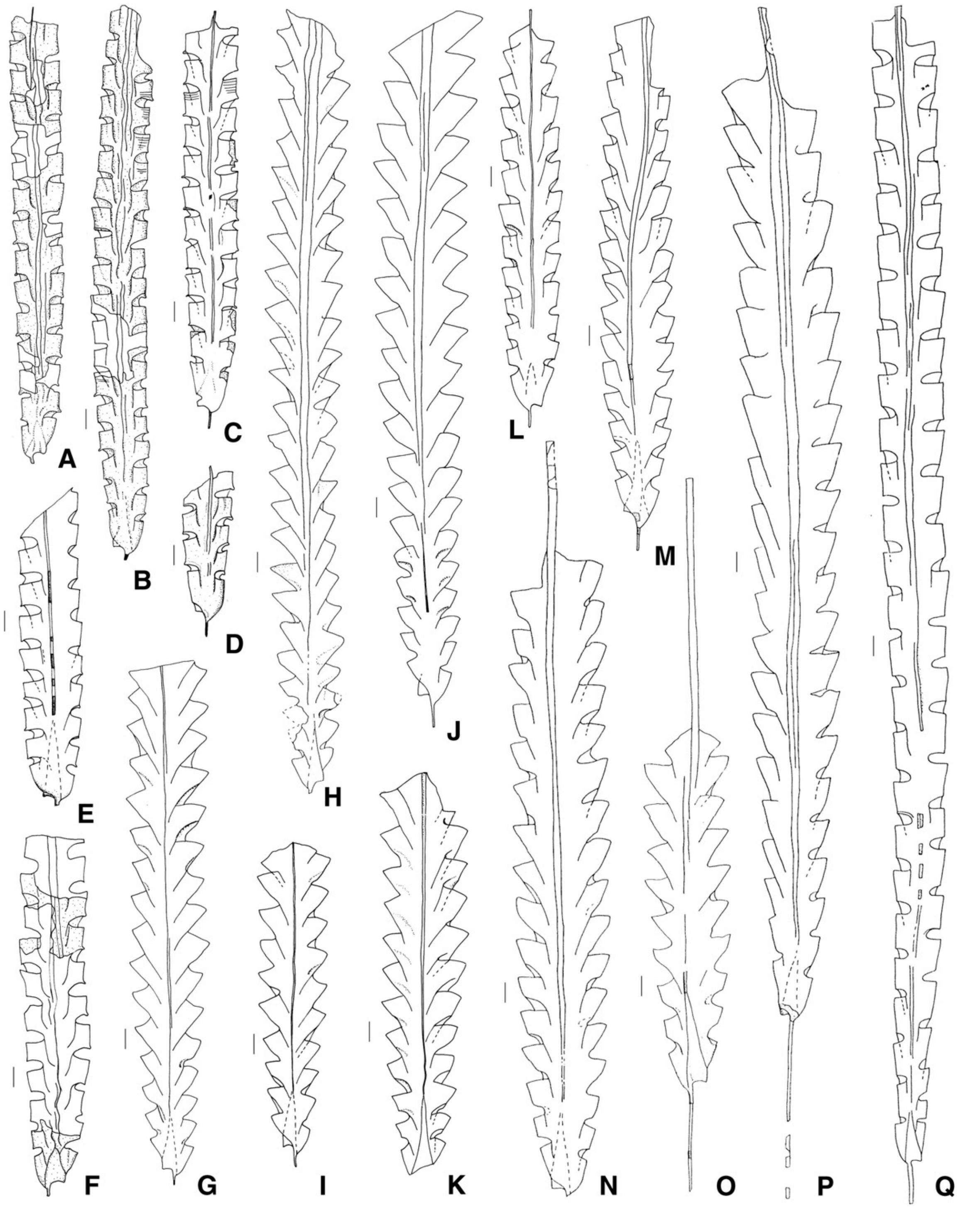

Fig. 5. Characteristic Hirnantian (latest Ordovician) graptolites from the lowermost part of the Sarchahan Formation at Kuh-e Faraghan; all specimens from the *Normalograptus persculptus* Zone. A–D. *Normalograptus ajjeri* (Legrand); A, CNIGR 1/13212, level MG10172; B–D, CNIGR 2/13212-4/13212, level MG10171. E. *Normalograptus medius* (Tornqist), CNIGR 5/13212, level MG10172. F. *Normalograptus* ex gr. *normalis* (Lapworth), CNIGR 6/13212, level MG10172. G–I. *Glyptograptus*? *laciniosus* (Churkin and Carter), CNIGR 7/13212-9/13212, level MG10171. J–K. *Glyptograptus*? *lungmaensis* (Sun), CNIGR 10/13212, 11/13212, level MG10171. L–M. *Normalograptus parvulus* (Lapworth), L, 12/13212, level MG10171; M, CNIGR 13/13212, level MG10172. N. *Normalograptus persculptus* (Elles and Wood), CNIGR 14/13212, level MG10171. O. *Glyptograptus lanpherei* (Churkin and Carter), CNIGR 15/13212, level MG10172. P. *Normalograptus wangjiawanensis* (Mu and Lin), CNIGR 16/13212, level MG10171. Q. *Normalograptus rhizinus* (Li and Yang), CNIGR 17/13212, level MG10172. Scale bars = 1 mm.

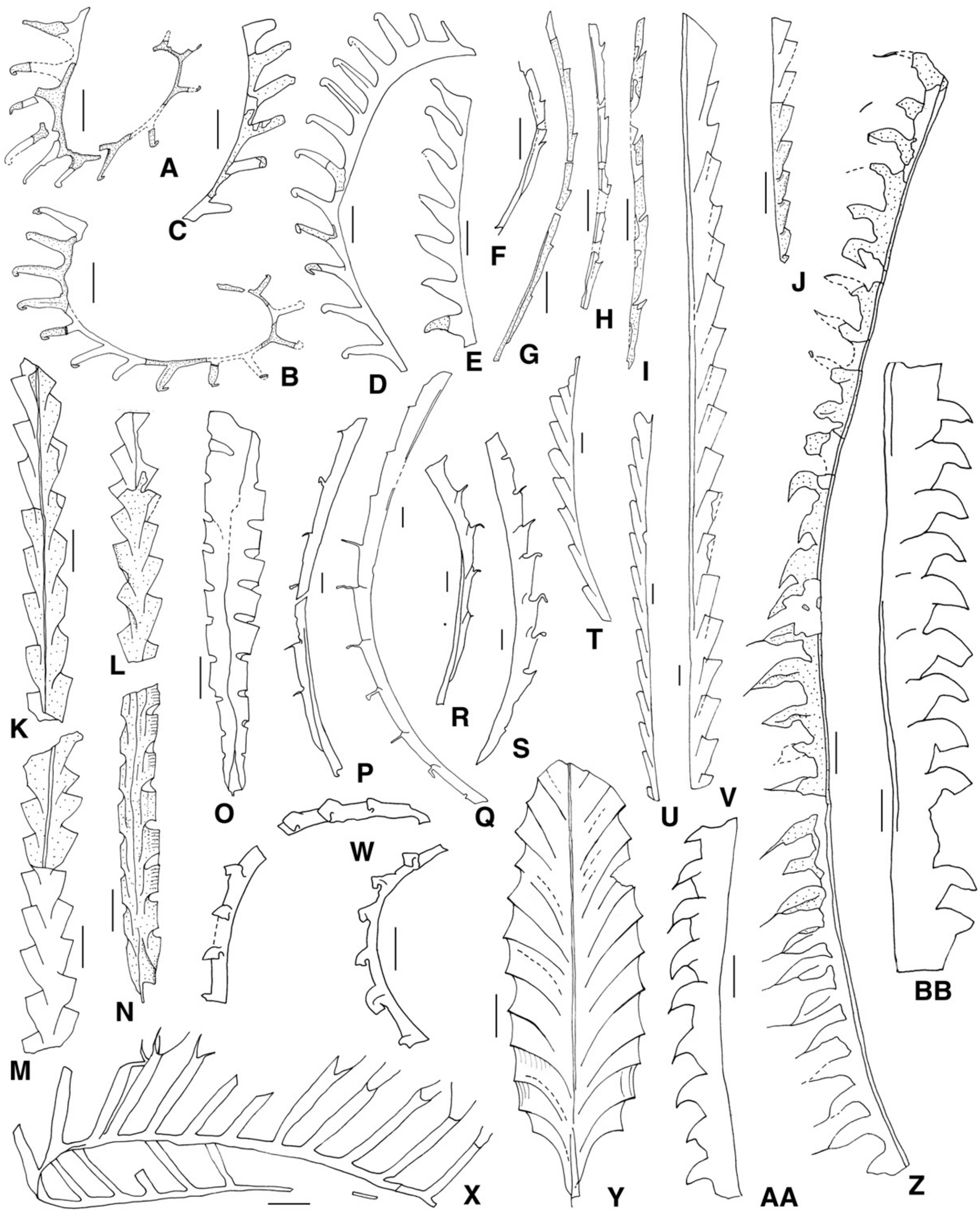

Fig. 6. Characteristic Aeronian (early Silurian) graptolites from the lower part of the Sarchahan Formation at Kuh-e Gahkum. A. *Demirastrites triangulatus triangulatus* (Harkness), CNIGR 18/13212, level MG10188a. B. *Demirastrites* cf. *praedecipiens* (Sudburi), CNIGR 19/13212, level MG10188a. C–E. *Demirastrites* ex gr. *triangulatus* (Harkness); C–D, CNIGR 20/13212-21/13212, fragments of various parts of rhabdosomes, level MG10187a; E, CNIGR 22/13212, level MG10188a. F–I. *Neolagarograptus* sp., CNIGR 23/13212-26/13212, level MG10188a. J. *Pristiograptus regularis* (Tornqist), CNIGR 27/13212, level MG10192. K–M, *Glyptograptus* ex gr. *tamariscus* (Nicholson); K. CNIGR 28/13212, level MG10187a; L–M. CNIGR 29/13212, 30/13212, level MG10188a. N. *Normalograptus* sp., CNIGR 31/13212, level MG10192, *Lituigraptus convolutus* Zone. O. *Neodiplograptus* cf. *sinuatus* (Nicholson), CNIGR 32/13212, level MG10188a. P–S. *Neolagarograptus tenuis* (Portlock), CNIGR 33/13212-36/13212, level MG10193. T–U. *Pribylograptus* ex gr. *argutus* (Lapworth), CNIGR 37/13212-38/13212, level MG10192. V. *Pristiograptus* ex gr. *variabilis* (Perner), CNIGR 39/13212, level MG10193. W.“*Monograptus*” cf. *gemmatus* (Barrande), CNIGR 40/13212, level MG10195. X. *Rastrites phleoides* Tornqist, CNIGR 41/13212, level MG10192. Y. *Petalolithus praecursor* Boucek and Přibyl, CNIGR 42/13212, level MG10192, *Lituigraptus convolutus* Zone. Z. *Lituigraptus convolutus* (Hisinger), CNIGR 43/13212, level MG10192. AA–BB. *Stimulograptus sedgwickii* (Portlock), CNIGR 44/13212-45/13212, level MG10195. Scale bars = 1 mm. A–I, K–M, O, *Demirastrites triangulatus* Zone; J, N, T, U, W–Z, *Lituigraptus convolutus* Zone; P–S, V, AA, BB, *Stimulograptus sedgwickii* Zone.

sandstones consist of subarkoses to subarkosic greywackes (Fig. 8B), although the latter are related to diagenetic alteration (or ‘secondary greywackization’).

The coarsening-up trend and progressive upward appearance of large bedforms of the lower sandstone packages represent progradation of shoal complexes, whereas the upper sandstone packages are interpreted to record the high energy of bedload under upper plane bed conditions on a foreshore to coastal plain. Both palaeoenvironments may be related to two episodes of delta-associated progradation of shoal complexes and coastal-plain settings, but a definitive reconstruction is precluded by the lack of laterally equivalent exposures.

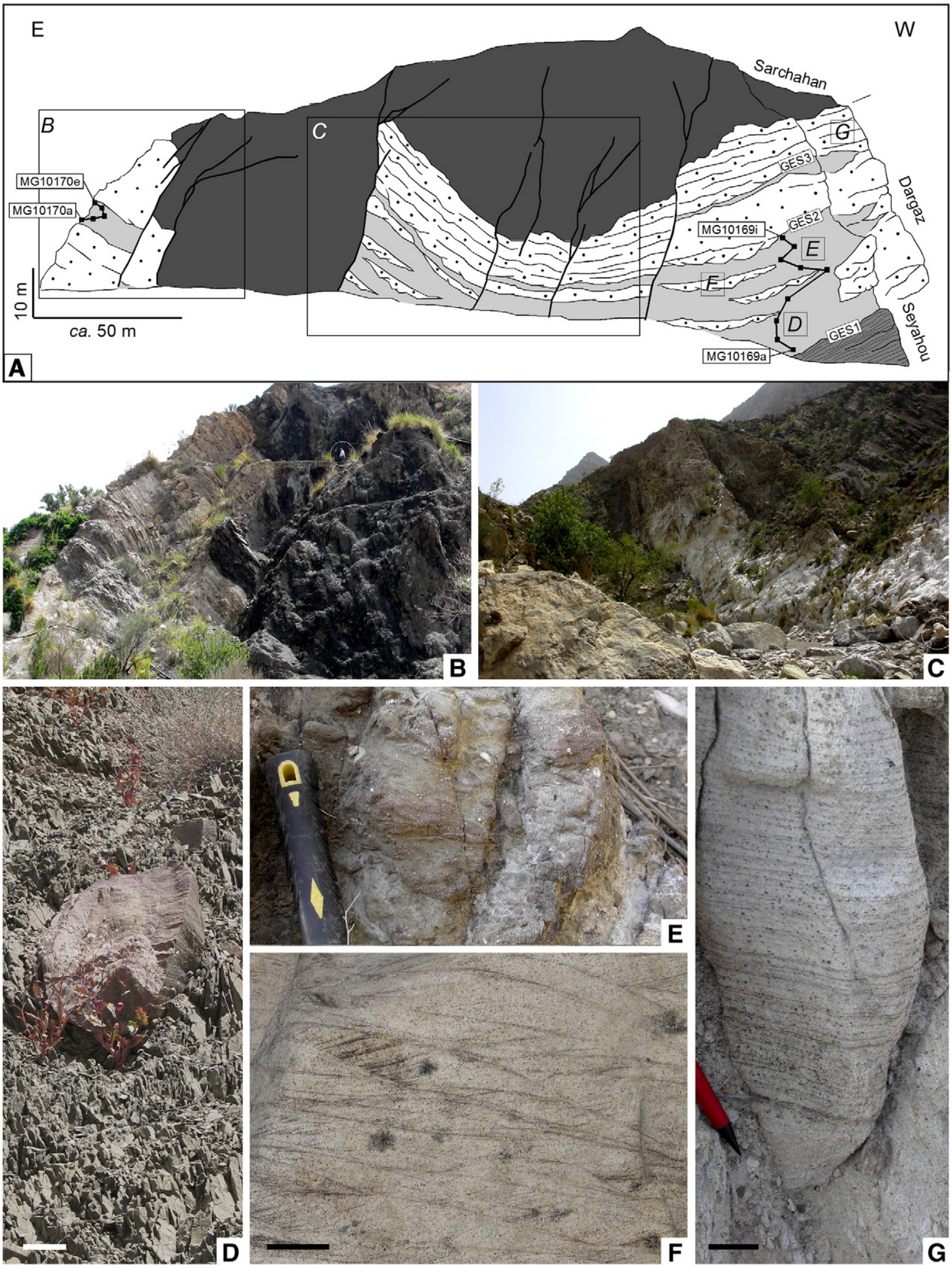

Fig. 7. Field aspect of the Dargaz and Sarchahan formations along the Pashagh valley, Kuh-e Faraghan. A. Sketch of the SE corner of Kuh-e Faraghan and setting of next pictures. B–C. Field details of previous sketch; encircled scale. D. Quartzitic lonestone embedded in the lower Dargaz diamictite. E. Crudely stratified, lower Dargaz diamictite. F. Cross-laminated sandstone infilling the channels that cut the lower Dargaz diamictite; scale = 4 cm. G. Parallel-laminated, upper Dargaz sandstone; scale = 5 cm.

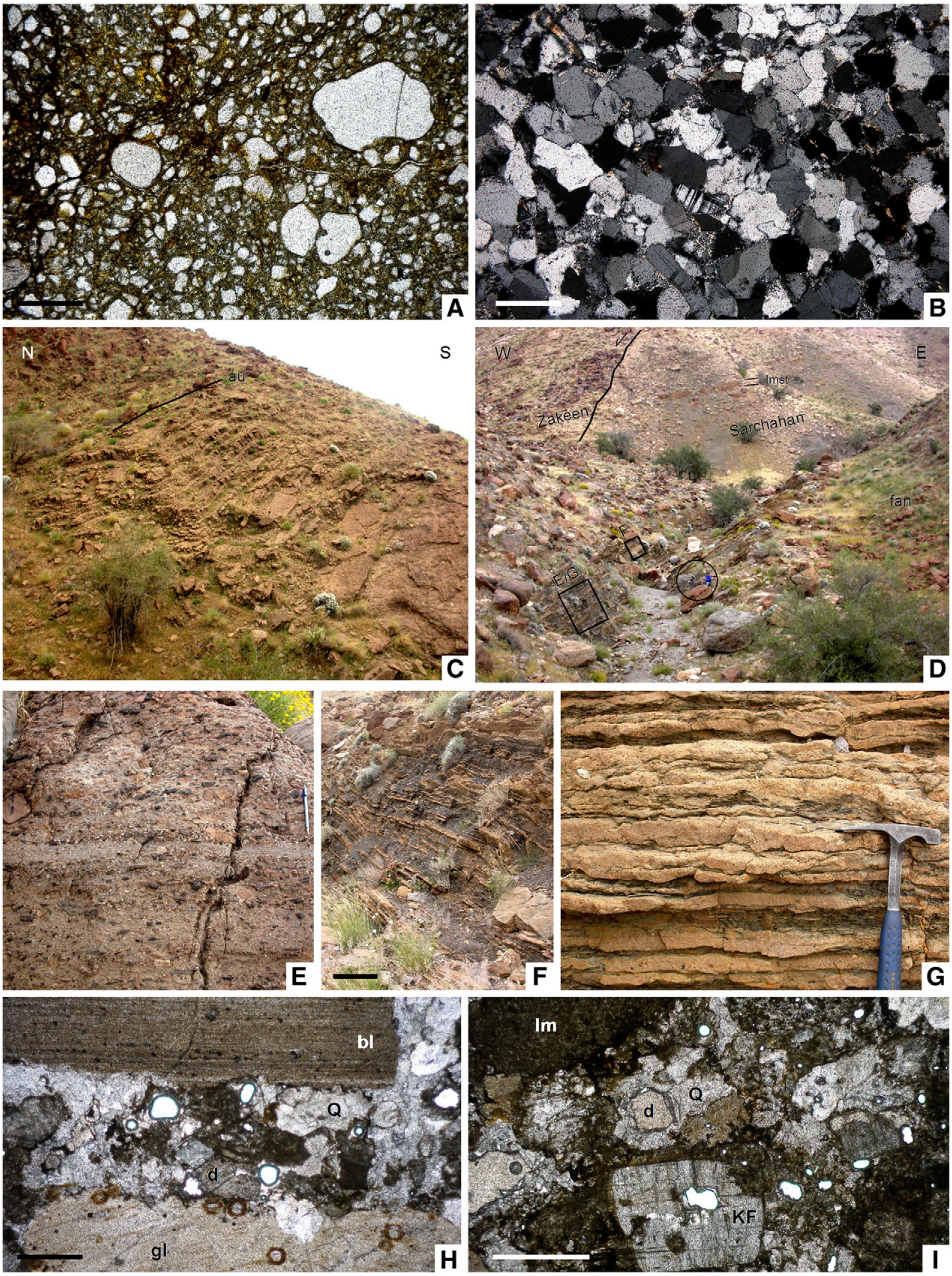

Fig. 8. A. Plane-polarised photomicrograph of the lower Dargaz, massively stratified diamictite from Kuh-e Faraghan; scale bar = 1 mm. B. Cross-polarised light photomicrograph of the lower Dargaz cross-bedded subarkose showing partial 'greywackization'; scale bar = 300 μm. C–D. Field aspect of the Sarchahan fan-shaped turbidite system in Kuh-e Gahkum and setting of next pictures; au: angular unconformity, lmst: limestone; encircled scale. E. Conglomeratic sheet-like beds of the Sarchahan basement (unnamed formation) in Kuh-e Gahkum. F. Turbidite conglomeratic litharenite/black shale couplets of the Sarchahan Formation; scale bar = 30 cm. G. Amalgamated Bouma (Ta) turbidites of the Sarchahan Formation. H–I. Plane-polarised light photomicrograph of the Sarchahan turbiditic conglomeratic litharenites; bl: black pyritic limestone, gl: grey limestone with pseudomorphs of hexagonal-outlined authigenic crystals, Q: quartz cement, d: dolomite rhombs, KF: K-feldspars; scale bars = 1 mm and 500 μm, respectively.

4.3. The Sarchahan Formation at Kuh-e Faraghan

The Dargaz/Sarchahan contact is marked by a scouring discontinuity and a sharp change in depositional systems. The latter consists of monotonous black and grey shales, which display local parallel laminae, and is enriched in organic matter with TOC values ranging from 4.6 to 5.0%. The formation is rich in graptolites and pyritic clusters and its lower part is devoid of bioturbation.

An essential condition for the formation of kerogenous black shales is the long-term depletion of oxygen in the marine bottom waters and the sediment itself, a condition supported by the general absence of burrowing and good preservation of graptolites. Such anoxic conditions can be either established by a widely restricted water circulation, extremely high rates of phytoplankton productivity, or a combination of both. The record of homogeneous mud under quiescent and anoxic conditions was a widespread process that took place throughout the North-African margin of Gondwana across the Hirnantian–Llandovery transition (Lüning et al., 2000,2005; Vecoli, 2008; Le Heron et al., 2009).

4.4. The Sarchahan Formation at Kuh-e Gahkum

Exposures of the Sarchahan Formation at Kuh-e Gahkum do not exceed 0.4 ha. They are bounded to the west by a fault and covered to the east by Quaternary deposits. The formation is unconformably underlain by a thick succession (>80 m) of thin- to thick-bedded, amalgamated conglomerate beds of uncertain age (Fig. 8E). These contain poorly sorted, polymictic clasts, up to 60 cm in size, dominated by brownish dolostone, black limestone, sandstone, shale, quartz, volcanoclast pseudomorph, and chert in variable proportions. Matrix composition displays the same mixture of clasts, although terrigenous claystone is dominant. The framework is irregularly cemented by intergranular poikilotopic dolomite, ferroan dolomite, and silica, which confer a generalised brownish stain to the whole unit. The carbonate composition of this unit has led some authors (Verrall, 1978) to refer the Sarchahan basement to the lower Cambrian Barut Formation (Stöcklin et al., 1964). However, the latter has been defined in the Alborz Mountains and it is preferable to avoid its application in the Zagros. The presence of black limestone clasts exhibiting parallel and low-angle laminae rife with pyrite crystals permits recognition of the erosion from a source rock typical of some Neoproterozoic–lowermost Cambrian salt-plug complexes scattered throughout the Zagros (Bosák et al., 1998; Rahnama Rad et al., 2008).

The overlying Sarchahan stratotype, ca. 170 m thick, can be subdivided into two distinct units or informal members. The lower member, 35 m thick, consists of a wedge of amalgamated conglomerate and conglomeratic sandstone strata passing laterally into gravel sandstone/black shale couplets (Fig. 8C–D and F). The thin-bedded alternations are laterally persistent at outcrop scale (10–20 m). Single polymictic litharenites, up to 12 cm thick, display scouring bases marked by sole, tool and flute marks (Fig. 8G). They are generally graded to chaotic (or massive) beds, although some are clearly graded (from gravel to siltstone) and even display crude low-angle lamination and asymmetric ripples at their top. The clasts are rounded to subangular and poorly sorted, and consist dominantly of quartz, quartzite, chert, K-feldspar, black pyritic limestone, dolostone, and shale (Fig. 8H–I). They are imbricated to chaotically arranged and have a matrix- to clast-supported fabric. Patches of poikilotopic dolostone and silica are present although less abundant than in the underlying unnamed formation. The top of the lower member is sharp and characterised by the disappearance of conglomerates and sandstones. Axes of scouring bases are oriented to the NE–ENE. The upper member, 135 m thick, consists of homogeneous black shales locally interrupted by metre-thick dolostone beds rife with brachiopods.

Although a complete sedimentological interpretation is precluded by the reduced extension of the Sarchahan exposures at Kuh-e Gahkum, some implications can be advanced. By comparison with the neighbouring Kuh-e Faraghan massif, the basement of the Sarchahan Formation at Kuh-e Gahkum is represented by an unnamed formation (probably pre-Floian in age due to the lack of the Floian–Katian Seyahou Formation and the conspicuous presence of clasts derived from the underlying salt-plug complexes) that played a palaeotopographic role during the Silurian transgression. At the beginning of the Llandovery, this palaeorelief became a passive source of erosion. It shed enough sediment to form a prominent fan-shaped clastic wedge of amalgamated conglomerate sheets, which are still preserved at the south-eastern part of the massif (the so-called 'unnamed' formation of Fig. 2B). Deposition of the laterally equivalent thin-bedded gravel sandstones that punctuated the autochthonous, low-oxygenated black shale background represents a slope-apron environment that episodically recorded the input of high-density turbulent flows. Graded beds display close affinities with classical Bouma (Ta) turbidites (Shanmugan, 1997), although a clear distinction with debris flows are not possible at the lowermost part of the Sarchahan Formation.

Trends in gravel sandstone/black shale ratio and sandstone thickness seem to be the most sensitive indicator of proximality. The ratio shows two coarsening upward trends in the first 30 m, finally followed by a homogeneous black shale package, representing an interval of quiet water and hemipelagic sedimentation. In summary, autochthonous low-oxygenated black shales alternate with thin-bedded turbidites that display a vertical proximal-to-distal trend representative of a decrease in basin relief. The basal turbidites originated close to a sediment source associated with the underlying (unnamed) amalgamated conglomerates and breccias. Three palaeogeographic possibilities can be invoked to explain the sharp increase of accommodation space related to the lower Sarchahan deep-sea fan: (i) the onset of block faulting increasing slope instability; (ii) the erosion of an inherited, high-relief, passive palaeotopography; or (iii) the onlapping infill of Hirnantian tunnel channels. The final burial of this palaeorelief is marked by deposition of the upper Sarchahan member, which represents the classical Llandovery kerogenous shales that blanketed North Gondwana.

5. Hirnantian event stratigraphy and palaeogeographic context

At Kuh-e Faraghan, the syn-glacial Dargaz strata rest with sharp unconformity upon the pre-glacial upper Seyahou Member (Fig. 2), Katian in age and represented by highly burrowed, rhythmically bedded tidalites. The Dargaz Formation displays a key succession of events: (i) a first regressive–transgressive cycle, marked by glaciogenic scouring into a pre-glacial (Katian) substrate and deposition of transgressive glaciomarine diacmictites; (ii) a second cycle, related to the progradation/retrogradation (or advance/retreat) of an ice front, as a result of which a shoal complex/glaciomarine diamictite couplet is recorded; and (iii) a third cycle that mimics the previous one, although its lower part is dominated by coastal plain deposits that were succeeded by a final deglaciation, which led to the definitive flooding of the platform and the record of the kerogenous Sarchahan black shales. The persistence of this flooding buried neighbouring palaeoreliefs, both in Kuh-e Faraghan and Kuh-e Gahkum. Another subdivision is plausible if we consider the sedimentary sequences bounded by major erosive boundaries or unconformities; in this case, the Dargaz-lower Sarchahan unit can be subdivided into transgressive–regressive cycles including GES1, GES2, GES3, and the Dargaz/Sarchahan erosive contact.

The erosive nature of the sandstone package bases probably implies deposition during glacial advances. No direct evidence for subglacial erosion (soft sediment striation) was found in or above the channelled deposits. Therefore, no evidence for major glacially related tunnel valleys was identified, although the reduced available exposures of the Dargaz Formation preclude their identification. However, evidence for scour of important local extent is recognised in Kuh-e Faraghan: the described unconformities that underlie the glacial depositional sequences may have been produced by the direct action of ice abrasion, meltwater, or a combination of both. A possible tunnel-channel shoulder may be preserved in Kuh-e Gahkum, where deposition of the fan-shaped Sarchahan turbidite system was sourced from an inherited palaeorelief that display distinct lithological features different to those recognised in Kuh-e Faraghan. Erosion of both source areas across the Hirnantian–Llandovery transition led to deposition of litharenites (rich in pre-Floian black pyritic limestones and dolostones) in the former and subarkoses in the latter.

Palaeocurrent measurements from the incisions recorded in the Dargaz Formation indicate a predominant north–northeast-dipping palaeoslope, which is in agreement with the orientation of the tunnel channels preserved in Saudi Arabia and Jordan (Vaslet, 1990; Clark-Lowes, 2005). Our data suggest the presence of an Hirnantian satellite ice cap neighbouring the Zagros. The magnitude of the Dargaz-related erosive incisions does not exceed the estimates of 45–80 m for the sea-level fluctuations associated with the Hirnantian glaciation, quoted in the literature (Le Heron and Dowdeswell, 2009; Le Heron et al., 2010). Neighbouring Hirnantian meltwater-produced incisions are recognised by mappable tunnel-channel incisions, ca. 4–6 km wide, 30–50 km long and 100 m deep, in Saudi Arabia (Vaslet, 1990; Clark-Lowes, 2005), Jordan (Powell et al., 1994; Turner et al., 2005), Libya (Le Heron et al., 2004), the Tassili N'Ajjer in Algeria (Hirst et al., 2002), Mauritania (Ghienne and Deynoux, 1998), and the Anti-Atlas of Morocco (Le Heron et al., 2007, 2008).

6. The Zagros Basin fringing the Arabian margin of Gondwana

Although the Arabian Plate is a tectonostratigraphic term widely used in early Palaeozoic palaeogeographic reconstructions, the "plate" came into existence only in the Oligocene. Since then, the rocks that comprise what is now the Arabian Peninsula, Syria, Jordan, Iraq, and the Iranian Zagros began to be separated from the African continent because of rifting along the margin of northeast Africa and the opening of the Red Sea and Gulf of Aden (Fig. 1A).

Throughout the Neoproterozoic to the end of the Palaeozoic, the Arabian "Plate" was part of Gondwana, so that we will refer below to the Arabian margin of Gondwana. The Zagros was located near the equator during the Neoproterozoic and, during the Cambrian–Ordovician, it followed the southward (and poleward) drift that characterised West and East Gondwana, reaching during Silurian times as far as ca. 60ºS latitude (Cocks and Torsvik, 2002; Heydari, 2008).

On the Arabian margin, the occurrence of Hirnantian glaciogenic rocks and tunnel valleys have been described in the Al Qasim district and the Wajid and Widyan plateaux of Saudi Arabia (McClure, 1978; Hughes-Clark, 1988; Vaslet, 1990; Clark-Lowes, 2005), as well as in the neighbouring southern desert of Jordan (Armstrong et al., 2005; Turner et al., 2005; Armstrong et al., 2009). The position of tunnel valleys and glacially scoured palaeoreliefs at the surface and the subsurface of Saudi Arabia suggest that the glaciated source area was located in the region of the Arabian and Arabian–Nubian Shields, and that sediment transport was toward the present-day east to northeast (Fig. 1A). Northwest Saudi Arabia formed part of a more extensive ice sheet of similar size than the present-day Antarctic ice sheet (Le Heron and Dowdeswell, 2009).

Current models for the Hirnantian glaciation in Jordan have recognised up to two major phases of glaciation (Abed et al., 1993), which are correlatable with two major glacial advances and retreats recorded in northwest Saudi Arabia (Vaslet, 1990; Al-Harbi and Mujtaba Khan, 2009) (Fig. 9). However, Turner et al. (2005) proposed a four-stage glacial model where the ice preferentially excavated fault-controlled depressions (reactivation of faults would be related to hydrothermal activity) cutting steep-sided U-shaped valleys. The forth glacial cycle of Jordan would be coeval to the second glacial phase of Saudi Arabia. Subsequently, the second glacial phase in Arabia has been reinterpreted by Miller and Mansour (2007), who described a more complex record of ice advance and retreat in the Sarah Formation. In a similar way, two major Hirnantian sequences have also been recognised in Spain (Álvaro and Van Vliet-Lanoë, 2009), Morocco (Loi et al., 2010), Mauritania (Ghienne, 2003), and Turkey (Monod et al., 2003), although in the two last regions, each major sequence has also been subsequently subdivided into two higher frequency cycles. Therefore, although the higher frequency cycles have not been widely recorded, the patterns of major ice advances interrupted by smaller-scale pulses have been interpreted as reflecting eccentricity and obliquity moderated ice volume changes (Sutcliffe et al., 2000; Armstrong et al., 2009).

A particularity of the Ordovician–Silurian transition in the Arabian margin was that the glacial incisions did not take place in a Gondwanan passive margin, like those recorded in northern Africa and southwestern Europe. Two Late Ordovician uplift episodes have been reported from Saudi Arabia: (i) a Katian episode in the Wajid plateau, documented by the uplift and deformation of the Dibsiyah Formation and the penecontemporaneous erosion of valley systems filled by the Sanamah Formation (Oterdoom et al., 1999); and (ii) a second uplift phase recognised across the Ordovician–Silurian boundary interval, marked in the same plateau by the onset of an angular unconformity separating the Sanamah Formation from the Qusaiba Member (Stump et al., 1993; Stump and Van der Eem, 1995). In addition, in the Lut Block of Central Iran, the Ordovician–Silurian

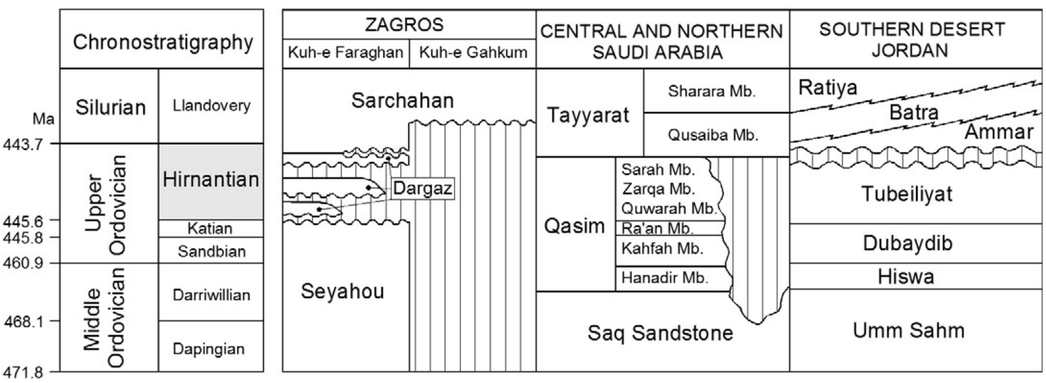

Fig. 9. Summarised chrono- and lithostratigraphic chart of the Zagros Mountains, Saudi Arabia, and Jordan, based on Vaslet (1990), Armstrong et al. (2005), Clark-Lowes (2005), Turner et al. (2005), and this work.

transition is associated with transtensive extension and syn-rift volcanism, as a result of which flood basalts of up to 500 m thick extended over 1000 km in areas that neighboured the Arabian margin and were an integral part of Gondwana during the Ordovician (Berberian and King, 1981; Husseini, 1990; Millson et al., 1996; Sharland et al., 2001; Bagheri and Stampfli, 2008; Torsvik and Cocks, 2009).

The abrupt end of the Hirnantian glaciation is marked by an extensive marine flooding that deposited organic-rich 'hot shales' across large areas of the Arabian Peninsula and northern Africa. The diachronous beginning of this final deglaciation provided the ideal conditions for deposition of kerogenous rocks. The reducing conditions at the seafloor were sufficient to produce and preserve organic matter rich in radioactive elements. This gives the distinctive 'hot' response of gamma ray logs. The Silurian base is a proven source for hydrocarbons throughout North Gondwana, from Morocco to the Zagros. As a result, the glacial events that affected the African-Arabian margin of Gondwana had a major impact on the petroleum and gas systems in the region, and resulted in the deposition of source rocks, all in the deglaciation phase, immediately following the final glaciation (Bell and Spaak, 2006). In Jordan, timing and model of black shale deposition is still controversial (Delabroye and Vecoli, 2010). For Armstrong et al. (2005), the basal black shales of the Batra Formation are Hirnantian in age and have been linked to freshening by deglacial meltwater. In contrast, Lüning et al. (2005) considered this unit as Rhuddanian (early Silurian) and related to nutrient enrichment of shallow marine environments by coastal upwelling.

7. Conclusions

The effects of the Hirnantian glaciation has been recognised in the Kuh-e Faraghan and Kuh-e Gahkum exposures of the Zagros Mountains. In the former, the glaciogenic strata have been grouped in the Dargaz Formation, a new lithostratigraphic unit that comprises three progradational/retrogradational sedimentary cycles (bounded by three glacial erosive surfaces), each potentially controlled by the regional advance and retreat of the Hirnantian ice sheet. The overlying Sarchahan black shales capped an inherited glaciogenic palaeorelief punctuated by several erosive unconformities. By contrast, the Dargaz Formation is absent in Kuh-e Gahkum, where the basement of the Sarchahan Formation consists of pre-Floian, amalgamated conglomerates rich in carbonate clasts and cements. The end of the glaciation led to the flooding of this palaeorelief, which was onlapped with interbedded turbidite sandstones and kerogenous black shales arranged in Bouma-type couplets.

Based on a study of chitinozoans, acritarchs and graptolites, the glaciomarine Dargaz diamictites are dated as Hirnantian, whereas the youngest Sarchahan black shales are diachronous throughout the Zagros, ranging from the Hirnantian *persculptus* to the earliest Aeronian (Llandovery) *triangulatus* zones. The diachronism is related to onlapping geometries capping an inherited glaciogenic palaeorelief that preserved different depth incisions and affected different source land areas, probably related to the development of a Hirnantian satellite ice cap.

Acknowledgements

The authors are grateful to Mark Harris (Milwaukee) and another anonymous referee for their critical and useful comments on the manuscript. This research has been financed by the Iranian Offshore Oil Company (IOOC). Support came from the National Museum of Wales, L.P. and M.G.; and the Golestan University. Gh. R. Zare and Yaser Sheikhan are thanked for field assistance.

Appendix A. Stratigraphy of the Dargaz Formation

Definition. The Dargaz Formation is here proposed as a new lithostratigraphic unit to include the sandstones and diamictites that lie between the lower Seyahou and upper Sarchahan formations. It is named after the village located at the outlet of the Pashagh valley, in the Kuh-e Faraghan massif, Zagros Mountains, Iran.

Stratotype. Pashagh valley, at the southeast corner of the Kuh-e Faraghan massif; geographical coordinates: N56° 29′ 05″, E27° 52′ 20″.

Lithology and thickness. Alternation, 10–70 m thick, of whitish, tabular and lenticular sandstones and greenish and brownish, structureless to crudely stratified diamictites, which form diamictite/sandstone couplets.

Contacts. The Seyahou/Dargaz contact is placed at the change from highly burrowed, thin-bedded, rhythmic claystone/sandstone couplets to either (i) structureless diamictites bearing centimetre- to decimetre-sized, outsized lonestones or (ii) metre-thick packages of fine-to coarse-grained sandstones, and represents an erosive unconformity where the magnitude of the gap increases south-westward at Kuh-e Faraghan. The upper contact with the overlying Sarchahan Formation is sharp and locally erosive, and lies at the change from metre-thick packages of fine- to coarse-grained sandstones below to black claystones above.

Fossils and age. Hirnantian acritarchs and chitinozoans yielded by the interbedded diamictites of the Dargaz Formation are listed in Table 1; the sampled fossiliferous beds are marked in Fig. 7A.

References

Abed, M.B., Makhlouf, I.M., Amireh, B.S., Khalil, B., 1993. Upper Ordovician glacial deposits in southern Jordan. Episodes 16, 316–328.

Afaghi, A., Salek, M.M. (eds.), 1977. Geological Map of Iran, South-Central Iran, sheet no. 5 (1/1,000,000). National Iranian Oil Company, Exploration and Production.

Ala, M.A., Kinghorn, R.R.F., Rahman, M., 1980. Organic geochemistry and source rock characteristics of the Zagros petroleum province, Southwest Iran. J. Petrol. Geol. 3, 61–89.

Alavi, M., 2004. Regional stratigraphy of the Zagros fold-thrust belt of Iran and its proforeland evolution. Am. J. Sci. 304, 1–20.

Al-Harbi, O.A., Mujtaba Khan, M., 2009. Source and origin of glacial paleovalley-fill sediments (Upper Ordovician) of Sarah Formation in central Saudi Arabia. Arab. J. Geosci. doi:10.1007/s12517-009-0097-2.

Alsharhan, A.S., Nairn, A.E.M., 1997. Sedimentary Basins and Petroleum Geology of the Middle East. Elsevier, Amsterdam. 978 pp.

Álvaro, J.J., Van Vliet-Lanoë, B., 2009. Late Ordovician carbonate productivity and glaciomarine record under quiescent and active extensional tectonics in NE Spain. In: Bassett, M.G. (Ed.), Early Palaeozoic Peri-Gondwana Terranes: New Insights from Tectonics and Biogeography: Geol. Soc., London, Spec. Publ., 325, pp. 117–139.

Armstrong, H.A., Turner, B.R., Makhlouf, I.M., Weedon, G.P., Williams, M., Al Smadi, A., Abu Salah, A., 2005. Origin, sequence stratigraphy and depositional environment of an upper Ordovician (Hirnantian) deglacial black shale, Jordan. Palaeogeogr. Palaeoclimat. Palaeoecol. 220, 273–289.

Armstrong, H.A., Abbot, G.D., Turner, B.R., Makhlouf, I.M., Bayawa, M.A., Pedentchouk, N., Peters, H., 2009. Black shale deposition in an Upper Ordovician–Silurian permanently stratified peri-glacial basin, southern Jordan. Palaeogeogr. Palaeoclimat. Palaeoecol. 273, 368–377.

Bagheri, S., Stampfli, G.M., 2008. The Anarak, Jandaq and Posht-e-Badam metamorphic complexes in central Iran: new geological data, relationships and tectonic implications. Tectonophysics 451, 123–145.

Bell, A., Spaak, P., 2006. Gondwana glacial events and their influence in the petroleum system in Arabia. AAPG International conference and exhibition, Perth, Australia, 5–8 Nov. 2006.

Berberian, M., King, G.C., 1981. Towards a paleogeography and tectonic evolution of Iran. Can. J. Earth Sci. 18, 210–265.

Berry, W.B.N., Boucot, A.J., 1972. Correlation of the Southeast Asian and Near Eastern Silurian rocks. GSA, Spec. Pap. 137, 1–65.

Bordenave, M.L., 2008. The origin of Permo-Triassic gas accumulations in the Iranian Zagros foldbelt and contiguous areas: a review of Palaeozoic petroleum systems. J. Petrol. Geol. 31, 3–42.

Bordenave, M.L., Burwood, R., 1990. Source rock distribution and maturation in the Zagros belt, provenance of the Asmari and Bangestan reservoir oil accumulations. Org. Geochem. 16, 369–387.

Bosák, P., Jaroš, J., Spudil, J., Sulovský, P., Václavek, V., 1998. Salt plugs in the Eastern Zagros, Iran: results of regional geological reconnaissance. GeoLines 7, 3–173.

Bouché, P.M., 1965. Chitinozoaires du Silurien s.l. du Djado (Sahara nigérien). Rev. Micropaléontol. 8, 151–164.

Butcher, A., 2009. Early Llandovery chitinozoans from Jordan. Palaeontology 52, 593–629.

Clark-Lowes, D.D., 2005. Arabian glacial deposits: recognition of palaeovalleys within the Upper Ordovician Sarah Formation, Al Qasim district, Saudi Arabia. Proceed. Geol. Ass. 116, 331–347.
Cocks, L.R.M., Torsvik, T.H., 2002. Earth geography from 500 to 400 million years ago: a faunal and palaeomagnetic review. J. Geol. Soc., London 159, 631–644.
Cramer, F.H., 1971. Distribution of selected Silurian acritarchs. An account of the palynostratigraphy and palaeogeography of selected acritarch taxa. Rev. Esp. Micropaleont. 1–203 no. extr. 1.
Da Costa, N.M., 1971. Quitinozoários silurianos de Iguarapé da Rainha, Estado do Para. Dep. Nacl. Prod. Miner. Div. Geol. Miner. Bolivia 255, 1–101.
Davoudzadeh, M., Lensch, G., Weber-Dierenbach, K., 1986. Contribution to the paleogeography, stratigraphy and tectonics of the Infracambrian and Lower Paleozoic of Iran. N. Jb. Geol. Paläont., Abh. 172, 245–269.
Delabroye, A., Vecoli, M., 2010. The end-Ordovician glaciation and the Hirnantian Stage: a global review and questions about Late Ordovician event stratigraphy. Earth-Sci. Rev. 98, 269–282.
Eisenack, A., 1931. Neue Mikrofossilien des baltischen Silurs, 1. Paläontol. Z. 13, 74–118.
Eisenack, A., 1963. Mitteilungen zur Biologie der Hystrichosphären und neue Arten. Palaeontographica Abt. A 118, 207–216.
Eisenack, A., 1968. Mikrofossilien eines Geschiebes der Borkholmer Stufe, baltisches Ordovizium F2. Mitteilungen aus dem Geologischen Staatsinstitut in Hamburg 37, 81–94.
Fensome, R.A., Williams, G.L., Barss, M.S., Freeman, J.M., Hill, J.M., 1990. Acritarchs and fossil prasinophytes: an index to genera, species, and infraspecific taxa. Am. Ass. Stratig. Palyn. Found. (AASP). Contr. Ser., 25, pp. 1–771.
Ghavidel-syooki, M., 1995. Introduction of the Sarchahan Formation as a new formation for Silurian sediments in the Zagros Basin, southern Iran. Geosci. Sci. Quart. J., Geol. Surv. Iran 15/16, 74–89.
Ghavidel-syooki, M., 2000. Biostratigraphy and palaeobiogeography of Late Ordovician and Early Silurian chitinozoans from Zagros Basin, Southern Iran. Hist. Biol. 15, 29–39.
Ghavidel-Syooki, M., 2008. Palynostratigraphy and palaeogeography of the Upper Ordovician Gorgan Schists (Southeastern Caspian Sea), Eastern Alborz Mountain Ranges, Northern Iran. Comunicacões Geológicas 95, 123–155.
Ghavidel-syooki, M., Khosravi, M.E., 1995. Investigation of Lower Palaeozoic sediments at Tang-e-Zakeen of Kuh Faraghan and introduction of Seyahou and Sarchahan formations in Zagros basin, southern Iran. Geosci. Sci. Quart. J. 4, 2–21.
Ghavidel-syooki, M., Winchester-Seeto, T., 2004. Chitinozoan biostratigraphy and palaeogeography of lower Silurian strata (Sarchahan Formation) in the Zagros Basin of Southern Iran. Mem. Ass. Austral. Palaeont. 29, 161–182.
Ghienne, J.F., 2003. Late Ordovician sedimentary environments, glacial cycles, and post-glacial transgression in the Taoudeni Basin, West Africa. Palaeogeogr. Palaeoclimat. Palaeoecol. 189, 117–145.
Ghienne, J.F., Deynoux, M., 1998. Large-scale channel fill structures in Late Ordovician glacial deposits in Mauritania, western Sahara. Sedim. Geol. 119, 141–159.
Ghienne, J.F., Boumendjel, K., Paris, F., Videt, B., Racheboeuf, P., Ait Salem, H., 2007. The Cambrian–Ordovician succession in the Ougarta Range (western Algeria, North Africa) and interference of the Late Ordovician glaciation on the development of the Lower Palaeozoic transgression on northern Gondwana. Bull. Geosci. 82, 183–214.
Ghienne, J.F., Monod, O., Kozlu, H., Dean, W.T., 2010. Cambrian–Ordovician depositional sequences in the Middle East: a perspective from Turkey. Earth-Sci. Rev. 101, 101–146.
Grahn, Y., 2006. Ordovician and Silurian chitinozoan biozones of western Gondwana. Geol. Mag. 143, 509–529.
Gutiérrez-Marco, J.C., Ghienne, J.F., Bernárdez, E., Hacar, M., 2010. Did the Late Ordovician African sheet reach Europe? Geology 38, 279–282.
Heydari, E., 2008. Tectonic versus eustatic controls on supersequences of the Zagros Mountains of Iran. Tectonophysics 451, 56–70.
Hirst, J.P.P., Benbakir, A., Payne, D.F., Westlake, I.R., 2002. Tunnel valleys and density flow processes in the upper Ordovician glacial succession, Illizi Basin, Algeria: influence on reservoir quality. J. Petrol. Geol. 25, 297–324.
Hughes-Clark, M.W., 1988. Stratigraphy and rock unit nomenclature in the oil-producing area of interior Oman. J. Petrol. Geol. 11, 5–60.
Husseini, M.I., 1990. The Cambro-Ordovician Arabian and adjoining plates: a glacio-eustatic model. J. Petrol. Geol. 13, 267–288.
Jacobson, S.R., Achab, A., 1985. Acritarch biostratigraphy of the Dicellograptus complanatus graptolite Zone from the Vaureal Formation (Ashgillian), Anticosti Island, Quebec, Canada. Palynology 9, 165–198.
Jardiné, S., Combaz, A., Magloire, L., Peniguel, G., Vachey, G., 1972. Acritarches du Silurien terminal et du Dévonien du Sahara algérien. 7th Int. Congr. Carboniferous Stratig. Geol., 1, pp. 295–311.
Jenkins, W.A.M., 1970. Chitinozoa from the Ordovician Sylvan shale of the Arbuckle Mountains, Oklahoma. Palaeontology 13, 261–288.
Jones, P.J., Stump, T.E., 1999. Depositional and tectonic setting of the Lower Silurian hydrocarbon source facies, central Saudi Arabia. AAPG Bull. 83, 314–332.
Konzalova-Mazankova, M., 1969. Acritarcha Evitt, 1963 aus dem unter–Ashgil Böhmens. Palaeontographica Abt. B 125, 81–92.
Le Heron, D.P., Dowdeswell, J.A., 2009. Calculating ice volumes and ice flux to constrain the dimensions of a 440 Ma North African ice sheet. J. Geol. Soc., London 166, 277–281.
Le Heron, D.P., Sutcliffe, O., Bourgig, K., Craig, J., Visentin, C., Whittington, R., 2004. Sedimentary architecture of Upper Ordovician tunnel valleys, Gargaf Arch, Libya: implications for the genesis of a hydrocarbon reservoir. GeoArabia 9, 137–160.
Le Heron, D.P., Ghienne, J.F., El Houicha, M., Khoukhi, Y., Rubino, J.L., 2007. Maximum extent of ice sheets in Morocco during the Late Ordovician glaciation. Palaeogeogr. Palaeoclimat. Palaeoecol. 245, 200–226.
Le Heron, D.P., Khoukhi, Y., Paris, F., Ghienne, J.F., Le Hérissé, A., 2008. Black shale, grey shale, fossils and glaciers: anatomy of the Upper Ordovician–Silurian succession in the Tazzeka Massif of eastern Morocco. Gondwana Res. 14, 483–496.
Le Heron, D.P., Craig, J., Etienne, J.L., 2009. Ancient glaciations and hydrocarbon accumulations in North Africa and the Middle East. Earth-Sci. Rev. 93, 47–76.
Le Heron, D.P., Armstrong, H.A., Wilson, C., Howard, J.P., Gindre, L., 2010. Glaciation and deglaciation of the Libyan Desert: the Late Ordovician record. Sedim. Geol. 223, 100–125.
Legrand, P., 2001. La faune graptolitique de la région d'In Azaoua (Tassili Oua-n-Ahaggar, confins Algéro-Nigériens). Ann. Soc. Géol. Nord 8, 137–158.
Loeblich Jr., A.R., 1970. Morphology, ulstrastructure and distribution of Paleozoic acritarchs. Proc. Am. Paleontol. Conv. Chicago, pp. 705–788.
Loeblich Jr., A.R., Tappan, H., 1976. Some new and revised organic-walled phytoplankton microfossil genera. J. Paleont. 50, 301–308.
Loeblich Jr., A.R., Tappan, H., 1978. Some Middle and Late Ordovician microphytoplankton frm central North America. J. Paleont. 52, 1233–1287.
Loi, A., Ghienne, J.F., Dabard, M.P., Paris, F., Botquelen, A., Christ, N., Elaouad-Debbaj, Z., Gorini, A., Vidal, M., Videt, B., Destombes, J., 2010. The Late Ordovician glacio-eustatic record from a high-latitude storm-dominated shelf succession: the Bou Ingarf section (Anti-Atlas, Southern Morocco). Palaeogeogr. Palaeoclimat. Palaeoecol. 296, 332–358.
Loydell, D.K., 2007. Graptolites from the Upper Ordovician and Lower Silurian of Jordan. Spec. Pap. Palaeontology 78, 1–66.
Lüning, S., Craig, J., Loydell, D.K., Štorch, P., Fitches, B., 2000. Lower Silurian 'hot shales' in North Africa: regional distribution and depositional model. Earth-Sci. Rev. 49, 121–200.
Lüning, S., Shahin, D., Loydell, H.T., Al-Rabi, A., Masri, B., Tarawneh, B., Kolonic, S., 2005. Anatomy of a world-class source rock: distribution and depositional model of Silurian organic-rich shales in Jordan and implications for hydrocarbon potential. AAPG Bull. 89, 1397–1427.
Mahmoud, M.D., Vaslet, D., Husseini, M.I., 1992. The Lower Silurian Qalibah Formation of Saudi Arabia: an important hydrocarbon source rock. AAPG Bull. 76, 1491–1506.
McClure, H.A., 1978. Early Paleozoic glaciation in Arabia. Palaeogeogr. Palaeoclimat. Palaeoecol. 25, 315–326.
McClure, H.A., 1988. The Ordovician–Silurian boundary in Saudi Arabia. Bull. Brit. Mus., Nat. Hist. (Geol.) 43, 155–163.
McGillivray, J.G., Husseini, M.I., 1992. The Paleozoic petroleum geology of Central Arabia. AAPG Bull. 76, 1473–1490.
Melvin, J., Sutcliffe, O.E., Ferebee, T., 2003. Origin and sedimentary infill of an Upper Ordovician (Ashgillian), glacial paleovalley near Tabuk, Northwest Saudi Arabia. Abstracts, 7th GEO Middle East Conference and Exhibition: Geol. Soc. London, October 2003, 90051.
Melvin, J., Miller, M.A., Sutcliffe, O.E., Ferebee, T.W., 2004. Post-glacial rebound unconformity within the Baq'a Member of the Sarah Formation (Ashgill): sequence stratigraphic implication at the Ordovician–Silurian boundary in Saudi Arabia. GeoArabia 9, 106.
Miller, M.A., Mansour, H.A.R., 2007. Preliminary palynological investigation of Saudi Arabian Upper Ordovician glacial sediments. Rev. Micropal. 50, 17–26.
Millson, J.A., Mercadier, C.G.L., Livera, S.E., Peters, J.M., 1996. The Lower Palaeozoic of Oman and its context in the evolution of a Gondwanan continental margin. J. Geol. Soc., London 153, 213–230.
Mobasheri, A., 2005. Sedimentological studies on the Seyahou and Sarchahan formations in Tang-e-Zakeen of Kuh-e-Faraghan at Bardar Abbas area, southern Iran. Nat. Iran. Oil Co., Sedim. Rep. 7, 1–56.
Molyneux, S.G., 1988. Late Ordovician acritarchs from northeast Libya. In: El-Arnauti, A., Owens, B., Thusu, B. (Eds.), Subsurface Palynostratigraphy of Northeast Libya: Garyounis Univ. Publ. , pp. 45–49.
Monod, O., Kozlu, H., Ghienne, J.F., Dean, W.T., Günay, Y., Le Hérissé, A., Paris, F., Robardet, M., 2003. Late Ordovician glaciation in southern Turkey. Terra Nova 15, 249–257.
Moscariello, A., Azzouni, H., Hulver, M., Alain, J., Rubino, J.L., 2008. New insights on the sedimentology and stratigraphy of the glaciogenic Late Ordovician Sanamah Member, Wajid Sandstone Formation, Southwest Saudi Arabia. AAPG Search and Discovery Article, #9077@2008 GEO 2008 Middle East Conference and Exhibition, Manama, Bahrain.
Nestor, V., 1980. Middle Llandoverian chitinozoans from Estonia. Eesti NSV Teaduste Academeia Keemia Geoloogia 29, 136–141.
Oterdoom, W.H., Worthing, M., Partington, M., 1999. Petrological and tectonostratigraphic evidence for a Mid Ordovician rift pulse on the Arabian Peninsula. GeoArabia 4, 467–500.
Paris, F., 1990. The Ordovician biozones of the North Gondwana domain. Rev. Palaeobot. Palynol. 66, 181–209.
Paris, F., Bourahrouh, A., Le Hérissé, A.L., 2000a. The effects of the final stages of the Late Ordovician glaciation on the marine palynomorphs (chitinozoans, acritarchs and leiospheres) in well NI-2 (NE. Algerian Sahara). Rev. Palaeobot. Palynol. 11, 87–104.
Paris, F., Verniers, J., Al-Hajri, S., 2000b. Ordovician chitinozoans from Central Saudi Arabia. In: Al-Hajri, S., Owens, B. (Eds.), Stratigraphic Palynology of the Palaeozoic of Saudi Arabia: Spec. GeoArabia Publ. (Gulf PetroLinh, Bahrain), pp. 42–56.
Paris, F., Le Hérissé, A., Monod, O., Kozlu, H., Ghienne, J.F., Dean, W.T., Vecoli, M., Gunay, Y., 2007. Ordovician chitinozoans and acritarchs from southern and southeastern Turkey. Rev. Micropal. 50, 81–107.
Powell, J.H., Kahlil, B.M., Masri, A., 1994. Late Ordovician–Early Silurian glaciofluvial deposits preserved in palaeovalleys in South Jordan. Sedim. Geol. 89, 303–314.
Rahnama Rad, J., Derakhsani, R., Farhoudi, G., Ghorbani, H., 2008. Basement faults and salt plug emplacement in the Arabian platform in Southern Iran. J. Appl. Sci. 8, 3235–3241.

Rickards, R.B., Wright, A.J., Hamedi, A.M., 2000. Late Ordovician and Early Silurian graptolites from southern Iran. Rec. West. Austral. Mus. Suppl. 58, 103–122.
Sarjeant, W.A.S., Stancliffe, R.P.W., 1994. The *Micrhystridium* and *Veryhachium* complexes (Acritarcha: Acantomorphitae and Polygonomorphitae): a taxonomic reconsideration. Micropaleontology 40, 1–77.
Senalp, M., Al-Laboun, A., 2000. New evidence on the Late Ordovician glaciation in Central Saudi Arabia. Saudi Aramco J. Techn. 11–40 Spring.
Senalp, M., Al-Ruwaili, M.H., Miller, M.A., 2002. New evidence on the stratigraphy of the Ordovician–Silurian boundary in Saudi Arabia. GeoArabia 7, 298–299.
Sepehr, M., Cosgrove, J.W., 2004. Structural framework of the Zagros fold-thrust belt, Iran. Mar. Petrol. Geol. 21, 829–843.
Shanmugan, G., 1997. The Bouma sequence and the turbidite mind set. Earth-Sci. Rev. 42, 201–229.
Sharland, P.R., Archer, R., Casey, D.M., Davies, R.B., Hall, S.H., Heward, A.P., Horbury, A.D., Simmons, M.D., 2001. Arabian Plate sequence stratigraphy. GeoArabia, Spec. Publ. 2, 1–369.
Sherkati, S., Letouzey, J., de Lamotte, D.F., 2006. Central Zagros fold-thrust belt (Iran): new insights from seismic data, field observation, and sandbox modelling. Tectonics 25, 1–27.
Staplin, F.L., Jansonius, J., Pocock, S.A.J., 1965. Evaluation of some acritarchous hystrichosphere genera. N. Jb. Geol. Paläontol. Abh. 123, 167–201.
Stöcklin, J., Ruttner, A., Nabavi, M.H., 1964. New data on the Lower Paleozoic and Pre-Cambrian of North Iran. Geol. Surv. Iran Rep. 1, 1–29.
Stockmans, F., Willière, Y., 1962. Hysrtrichophères du Dévonien belge (sondage de l'Asile d'aliénés à Tournai). Bull. Soc. Belge Géol. Paléontol. Hydrol. 71, 41–77.
Štorch, P., Massa, D., 2003. Biostratigraphy, correlation, environmental and biogeographic interpretation of the Lower Silurian graptolite faunas of Libya. In: Salem, M.J., Oun, K.M. (Eds.), The Geology of Northwest Libya. Vol. 1. Sedimentary Basins of Libya: 2nd Symp. Earth Sci. Soc. Libya, Tripoli, pp. 237–251.
Štorch, P., Massa, D., 2006. Middle Llandovery (Aeronian) graptolites of the Western Murzuq Basin and Al Qarqaf Arch Region, South–West Libya. Paleontology 49, 83–112.
Stump, T.E., Van der Eem, J.G., 1995. The stratigraphy, depositional environments and periods of deformation of the Wajid outcrop belt, southwestern Saudi Arabia. J. Afr. Earth Sci. 21, 421–441.
Stump, T.E., Connally, T.C., Van der Eem, J.G.L., 1993. The ?Late Precambrian to Early Triassic stratigraphy of the Kingdom of Saudi Arabia. Saudi Aramco Miscell. Geol. Rep. 1014.
Sutcliffe, O.E., Dosdeswell, J.A., Whittington, R.J., Theron, J.N., Craig, J., 2000. Calibrating the Late Ordovician glaciation and mass extinction by the eccentricity cycles of Earth's orbit. Geology 28, 967–970.
Torsvik, T.H., Cocks, L.R.M., 2009. The Lower Palaeozoic palaeogeographical evolution of the northeastern and eastern peri-Gondwanan margin from Turkey to New Zealand. In: Bassett, M.G. (Ed.), Early Palaeozoic Peri-Gondwana Terranes: New Insights from Tectonics and Biogeography: Geol. Soc., London, Spec. Publ., 325, pp. 3–21.
Turner, B.R., Makhlouf, I.M., Armstrong, H.A., 2005. Late Ordovician (Ashgillian) glacial deposits in southern Jordan. Sedim. Geol. 181, 73–91.
Vandenbroucke, T.R.A., Gabbott, S.E., Paris, F., Aldridge, R.J., Theron, J.N., 2009. Chitinozoans and the age of the Soom Shale, an Ordovician black shale Lagerstätten, South Africa. J. Micropal. 28, 53–66.
Vaslet, D., 1989. Late Ordovician glacial deposits in Saudi Arabia: a lithostratigraphic revision of the early Palaeozoic succession. Prof. Pap., Saudi Arab. Dep. Min. Miner. Res. 3, 13–44.
Vaslet, D., 1990. Upper Ordovician glacial deposits in Saudi Arabia. Episodes 13, 147–161.
Vavdrová, M., 1966. Palaeozoic microplankton from central Bohemia. Cas. Mineral. Geol. 11, 408–414.
Vecoli, M., 1999. Cambro-Ordovician palynostratigraphy (acritarchs and parasinophyts) of the Hassi-R'Mel area and northern Rhadames Basin, North Africa. Palaeontogr. Italica 86, 1–112.
Vecoli, M., 2008. Fossil microphytoplankton dynamics across the Ordovician–Silurian boundary. Rev. Palaeobot. Palynol. 91, 91–107.
Vecoli, M., Le Hérissé, A., 2004. Biostratigraphy, taxonomic diversity, and patterns of morphological evolution of Ordovician acritarchs (organic-walled microphytoplankton) from the northern Gondwana margin in relation to palaeoclimatic and palaeogeographic changes. Earth-Sci. Rev. 67, 267–311.
Verrall, D., 1978. The significance of thickness variations in the Gachsaran formation. NIOC Exploration report 182.
Webby, B.D., Cooper, R.A., Bergstom, S.M., Paris, F., 2004. Stratigraphic framework and time slices. In: Webby, B.D., Droser, M.L., Percival, I. (Eds.), The Great Biodiversity Event. Columbia Univ. Press, New York, pp. 41–47.
Wolfart, R., 1981. Lower Paleozoic rocks of the Middle East. In: Holland, C.H. (Ed.), Lower Paleozoic Rocks of the Middle East, Eastern and Southern Africa, and Antarctica. John Wiley & Sons, Chichester, pp. 6–130.
Xu, C., Jun-Xuan, F., Melchin, M.J., Mitchell, C.E., 2005. Hirnantian (latest Ordovician) graptolites from the Upper Yangtze region, China. Palaeontology 48, 235–280.